

Creating a New Malaria Vaccine Design that uses a Blood Stage *P. falciparum* Chassis for Non-Blood  
Stage Antigen Presentation

by

Shelbi Nicole Parker

B.S. Biomedical Engineering  
University of Texas at Dallas, 2017

Submitted to the Department of Biological Engineering in Partial Fulfillment of the Requirements for the  
Degree of

MASTER OF ENGINEERING IN BIOLOGICAL ENGINEERING

at the

MASSACHUSETTS INSTITUTE OF TECHNOLOGY

May 2022

©2022 Massachusetts Institute of Technology. All rights reserved.

The author hereby grants to MIT permission to reproduce and to distribute publicly paper and electronic  
copies of this thesis document in whole or in part in any medium now known or hereafter created.

Signature of Author: \_\_\_\_\_

Shelbi N. Parker  
Department of Biological Engineering  
May 13, 2022

Certified by: \_\_\_\_\_

Jacquin C. Niles  
Professor of Biological Engineering  
Thesis Supervisor

Accepted by: \_\_\_\_\_

Katharina Ribbeck  
Professor of Biological Engineering  
Graduate Program Committee Chair

# **Creating a New Malaria Vaccine Design that uses a Blood Stage *P. falciparum* Chassis for Non-Blood Stage Antigen Presentation**

by

Shelbi Nicole Parker

Submitted to the Department of Biological Engineering on May 13<sup>th</sup>, 2022, in Partial Fulfillment of the Requirements for the Degree of Master of Engineering in Biological Engineering

## **Abstract**

Malaria is a global disease that affects millions annually and the complex life cycle of the *Plasmodium* species that cause malaria results in increasing drug resistance and poor vaccine efficacy. Current vaccine designs focus on a single stage in the parasite life cycle and antibody responses are inefficient in offering protection, leading to “malaria rebound” as a lack of immune response to multiple stages of the life cycle result in case numbers returning to their levels before intervention. In this work, we utilize a blood stage parasite to present infection and transmission stage antigens. Plasmids using the conditional translation repressor system TetR-DOZI were created, and transgenic parasites that express the scaffold protein eTRAMP4 fused to either CSP or P25 were generated. We assessed the transgenic parasites for growth defects, proper fusion length, and localization to the parasitophorous vacuolar membrane. We also removed parasites from host red blood cells and examined two purification methods in the pipeline of developing a pure, intact culture of transgenic parasites. The methods and results of this work set the stage for a new malaria vaccine design that has the potential to fill the gap of current vaccine technologies.

Thesis supervisor: Jacquin Niles

Title: Professor of Biological Engineering

## **Acknowledgements**

First, I'd like to thank my advisor, Jacquin Niles, for his guidance in science and writing. His thoughtfulness and care for the project helped me finish this work as much as I could. I am very grateful for his advice and support.

Thank you to the National Science Foundation's Graduate Research Fellowship Program and the Alfred P. Sloan Foundation, who helped fund my graduate studies. I appreciate the network of support and the opportunity to impact the field that comes with these programs.

Thank you to Michael Birnbaum for serving as the head of my committee and for advocating for my health and wellbeing.

Special thanks to Charisse Flerida Pasaje, Lisl Esherick, and Kyle Jarrod McLean for making this project possible. They helped form the foundation of my knowledge in the lab, guided me in plasmid creation and troubleshooting, taught me invaluable tissue culturing skills, and let me use them as springboards for ideas.

To my colleagues in the Niles lab: you created a bustling, kind, and friendly environment that promoted my growth scientifically and personally. I'm grateful for the time we spent together in and out of lab and having been able to get to know such smart, fun, and giving people.

Thank you to my friends outside of academia who kept me grounded and let me talk way too much about parasites.

Finally, I cannot say enough how thankful I am for having my husband, Eske Pedersen, in my life. Thank you for the unwavering support, confidence in my abilities, and inspiring me to be better. A special thank you also goes to our dog, Henrietta, for being incredibly supportive and warming my feet during the writing process.

## Table of Contents

Abstract .....	2
Acknowledgements .....	3
Chapter I: An Introduction into Malaria and the Vaccine Landscape .....	9
Abstract .....	9
Drug Resistance to Malaria is a Growing Issue.....	9
The Complicated Life of <i>Plasmodium</i> Requires Multiple Points of Intervention .....	10
Vaccine Attempts Have Yet to Yield True Protection .....	12
Proposal for a New Malaria Vaccine Design.....	13
Chapter I References .....	15
Chapter II: Expressing Antigens outside their Native Contexts.....	18
Abstract .....	18
Introduction.....	18
Methods .....	21
Results and Discussion.....	25
Fusing Antigens to Scaffold Does Not Affect Parasite Growth.....	25
Confirmation of eTRAMP4-CSP and eTRAMP4-P25 fusion protein expression .....	26
eTRAMP4-CSP localizes to the parasitophorous vacuolar membrane (PVM).....	27
Conclusions.....	27
Chapter II References .....	29
Chapter III: Preparing Parasites for Use as a Aseptic Vaccine .....	31
Abstract .....	31
Introduction.....	31
Methods .....	33
Results and Discussion.....	36
Isolating Parasites from RBC Hosts using Protease Inhibitor E64 .....	36
Assessment of Purification via Giemsa Stain.....	36
Assessment of Purification via Immunofluorescence .....	40
Assessment of Purification via ELISA .....	41
Conclusions.....	43
Chapter III References .....	46
Chapter IV: Conclusions and Future Directions.....	47

## Table of Figures

- Figure 1. A graphical representation of the life cycle of *Plasmodium falciparum*.** The infection stage for a human host begins with an uninfected human serving as a blood meal for an infected *Anopheles* mosquito. Sporozoites from the infected mosquito's salivary glands travel through the skin to the liver where they develop into exo-erythrocytic schizonts that replicate inside hepatocytes. The blood stage begins once the parasites egress from the liver as merozoites and into the circulatory system to begin an asexual intra-erythrocytic development cycle--changing phases from rings to trophozoites to schizonts that will degrade the RBC membrane and explode out for new merozoites to invade nearby RBCs. The transmission stage starts from a few parasites that differentiate from blood stage phases into gametocytes; these gametocytes can be taken up by an uninfected *Anopheles* mosquito during a blood meal where they will replicate in the mosquito midgut before producing sporozoites that will transmit malaria to another human host. Created with BioRender.com..... 11
- Figure 2. Graphical table of different forms parasites can take in the human host or mosquito vector.** This graphical table lists example proteins found on the surface of the parasite and whether or not it has just a PPM or a PPM and a PVM. Created with BioRender.com. .... 12
- Figure 3. A graphical representation of the proposed malaria design for this work: EPAPs or engineered parasites for antigen presentation.** As a proof of concept, this design features an intact blood stage parasite acting as a chassis to present an antigen from another stage in the life cycle, either an infection stage antigen or a transmission stage antigen. Created with BioRender.com. .... 14
- Figure 4. A graphical representation of the two antigens for the proof-of-concept: CSP (left) and P25 (right).** (a) A representation of a sporozoite that shows the orientation of the circumsporozoite protein in the exterior leaflet of the parasite plasma membrane (PPM). (b) A representation of the wild type CSP sequence that features (from N terminus to C terminus) a signal peptide, Region I (RI), a central repeat region, Region II (RII), and a GPI anchor that anchors the protein into the PPM. (c) A representation of an ookinete that shows the orientation of the P25 in the exterior leaflet of the parasite plasma membrane (PPM). (d) A representation of the wild type P25 sequence that features (from N terminus to C terminus) a signal peptide, four epidermal growth factor-like domains (EGFLs), and a GPI anchor that anchors the protein into the PPM. Created with BioRender.com. .... 19
- Figure 5. Graphical representation of blood stage parasite membranes and the scaffold protein.** The scaffold protein natively sits in the outer leaflet of the PVM (inset left) while the transgenic parasites would express a fused antigen to this scaffold (inset right). The PVM surrounds the PPM for blood stage parasites. Created with BioRender.com..... 20
- Figure 6. Vector design and translational repressor system.** Vector designs for (A) protein scaffold and the (B) protein fusion utilize the pSN054 backbone. (C) The translational repressor system with TetR-DOZI in the absence and presence of an analog to tetracycline, aTc, is used to conditionally express proteins in transgenic parasite lines. (A) and (B) created with BioRender.com..... 21
- Figure 7. Imagined design of presenting antigens on scaffold protein on the blood stage parasite surface.** Created with BioRender.com..... 21

- Figure 8. Parasite growth without aTc (left) and with aTc (right) as measured via luminescence over 96 hours (2 IDCs) for eTRAMP4 constructs.** The eTRAMP4 scaffold alone is depicted in black, protein fusion with CSP in green, and protein fusion with P25 in blue..... 25
- Figure 9. Western blots for eTRAMP4 constructs using an HA tag without (-) and with (+) aTc present in culture media.** The top row of images corresponds to those probed for the HA tag at the end of the scaffold or fusion ( $\alpha$ -HA) and the bottom row corresponds to  $\alpha$ -GAPDH, which is a loading control and runs at approx. 36kD. The scaffold alone runs at approx. 20kD, the fusion with CSP runs at approx. 75kD, and the fusion with P25 runs at approx. 37kD. .... 26
- Figure 10. Immunofluorescence images of parasites in ring or schizont stages in merozoites for 3 parasite lines with and without aTc taken using fluorescent microscopy.** The pCRISPR line, that is the background into which the plasmids are transfected, does not contain the gene for the HA tag that should fluoresce in the FITC channel, and thus serves as a negative control. DAPI = nucleus, FITC = HA tag at the end of the scaffold or fusion, MITO = mitochondria, Merge = merged images, and Merge+POL = merged images overtop a polarized image of the infected RBC..... 28
- Figure 11. A simplified diagram of the current understanding of parasite egress from RBCs and pathway inhibitions.** (Top) Under normal conditions, parasites at schizogony use two different set of proteases: one set to degrade the RBC membrane and one set to degrade the PVM, which releases merozoites to infect new RBCs. (Middle) With the addition of leupeptin, the degradation of the RBC membrane is inhibited but the PVM degradation is not, resulting in free merozoites within an RBC. (Bottom) With the addition of E64, RBC membranes are degraded as normal but PVM degradation is inhibited, resulting in merozoites trapped within a PVM..... 32
- Figure 12. Graphical representation of Percoll (top) and MACS (bottom) workflows for purification of schizonts for de-ghosting with E64.** Percoll separates schizonts from other cells via discontinuous gradient centrifugation and isolated schizonts are then washed to remove Percoll carry-over. MACS magnetically separates late trophozoites and schizonts from other cells due to their paramagnetic nature, after which they are eluted from the filter and washed to remove any other potential carry-over. .... 33
- Figure 13. Grid of Giemsa stains for CSP- and P25-transgenic parasites, before and after incubation with 10 $\mu$ M E64 for at least 8 hours.** Parasites stain purple while RBCs stain a light red/brown color. For both parasite lines, before E64 is applied (left column) schizonts can be seen inside erythrocytes. After E64 incubation (right column), schizonts do not have a present RBC surrounding them, akin to the formation of PEMS as seen in Salmon's work. .... 37
- Figure 14. Grid of CSP- and P25-transgenic parasite lines (top and bottom, respectively) pre-purification via MACS or Percoll and pre-exposure to E64, as well as under various combinations of these conditions.** MACS-purified parasites have a larger number of parasites by the inclusion of late trophozoites in addition to schizonts, compared to Percoll-purified parasites. Percoll-purified parasites do seem to have more shearing that causes parasite debris not belonging to the enclosed body of a PEMS. .... 38
- Figure 15. Comparison between purification methods using immunofluorescent assays.** A two-part grid of immunofluorescence assays (top set = Percoll-purified and bottom set = MACS-purified) done on the parental line pCRISPR (top row), CSP-transgenic parasites (middle row), and P25-transgenic parasites (bottom row) where parasites were stained for nuclear content (far-left column),

glycophorin A and the HA tag (middle-left column). Also included are bright field images of the cells (right-middle column) and the three channels merged together (far-right column). DAPI = nuclear content. FITC = glycophorin A and HA tag. POL = bright field image. Merge = all three channels merged. .... 39

**Figure 16. Comparisons between blood standard curves and calculated contaminants using 4PL.** A grid of 4-parameter logistic curves for Percoll-purified (left column) and MACS-purified (right column) for parental parasite line pCRISPR (top row), CSP-transgenic parasites (middle row), and P25-transgenic parasites (bottom row). Grey triangles are the measured optical density (OD) values for known blood concentrations and the grey dashed line is the 4PL fitted curve to these points. Samples of parasites (n = 3) that have the concentrations calculated by the inverse 4PL are represented by blue, purple, and orange circles. Only sample points that fall within the linear region (between the A and D values of the 4PL) are shown on the graphs. .... 44

**Figure 17. Grid of comparisons between different ELISA 4PLs for Percoll-purified (left column) and MACS-purified (right column) samples.** Blood standards (top row) are compared between the 4PL curves for pCRISPR (black solid line), CSP (blue dashed line) and P25 (orange dot-dashed line). Samples (bottom row) compare the calculated values for the estimated number of RBCs contaminating parasites, where values are plotted only if their optical density is between their respective A and D. .... 45

## Table of Tables

<b>Table 1. List of plasmid assembly sequences for the eTRAMP4 scaffold and the two antigens, CSP and P25. ....</b>	<b>22</b>
<b>Table 2. List of equations for ELISA calculations. A is the value at 0 cells, D is the value at infinite cells, C is the point of inflection, and B is the Hill coefficient. ....</b>	<b>41</b>
<b>Table 3. Range of estimated RBCs contaminating parasite samples using inverse 4PL. M is the number of samples that were able to be estimated from optical densities that fell within their respective A and D. ....</b>	<b>42</b>



## Chapter I: An Introduction into Malaria and the Vaccine Landscape

### Abstract

Malaria affects millions of people annually and is caused by the transmission and replication of parasites of the genus *Plasmodium* in a human host. Parasites are injected into a human host during a mosquito blood meal as sporozoites which then sequester into the liver to replicate. After undergoing developmental changes in the liver, parasites then burst from hepatocytes as merozoites to invade and asexually reproduce in erythrocytes; a fraction of these will differentiate into gametocytes that can be taken up by a new mosquito during a blood meal where parasites develop in the mosquito midgut. These parasites are transmitted to another host when the newly infected mosquito bites a human host for a blood meal. *Plasmodium* at each of these stages express different surface antigens, which creates challenges for designing strategies to elicit fully protective immune responses. Current malaria vaccines focus on individual stages in the life cycle, have the potential for “malaria rebound”, and are inefficient in offering protection. I propose a multi-stage approach where a whole parasite serves as a chassis for protein presentation to reap the benefits of specific, chosen antigens.

### Drug Resistance to Malaria is a Growing Issue

Malaria is a global disease resulting in an estimated 240 million cases yearly<sup>1</sup>, afflicting large regions of the world including Africa, Southeast Asia, the Eastern Mediterranean, South and Central America, and the Pacific. The high burden of disease weighs most heavily on the African continent and the perpetrator is the parasite *Plasmodium falciparum* (Pf), which accounts for 99.7% of cases in this region<sup>1,2</sup>. Some success in reducing malaria incidence has been made via preventative measures such as insecticide-treated bed nets (ITNs), indoor residual spraying (IRS), and antimalarial drugs.

Between 2000 and 2015, ITNs were a widespread intervention method, averted an estimated 663 million clinical cases<sup>3</sup>. However, many factors hinder ITNs’ ability to consistently reduce malaria case numbers including insecticide resistance in Anopheline mosquitos<sup>4,5</sup>, damage to the nets such as holes<sup>1,6,7</sup>, and disruption in ITN deployment services<sup>1,4,6</sup>. IRS usage in sub-Saharan Africa resulted in varied levels of population protection, depending on the insecticide class, but prevented an estimated peak of 33 million cases in 2012 following publication of the WHO’s global plan for insecticide resistance management<sup>8</sup>. Protected numbers decreased over time to 21 million by 2017, in large part due to increasing resistance to many insecticides<sup>5,9</sup> but also due to mono-treatments in national-level insecticide IRS efforts<sup>8</sup>, allowing for development of resistance to the single insecticide used<sup>10</sup>. Anti-malarials such as chloroquine, sulfadoxine-pyrimethamine and artemisinin combination therapies that were once primary treatment options are losing effectiveness as *Plasmodium falciparum* gains drug resistance due to mutations<sup>11-14</sup>. With resistance causing waning efficacy of malaria treatment and prevention methods, alternative methods need to be considered.

Vaccines have been used globally to control disease severity and reduce case numbers for many diseases such as small pox, polio, mumps, and COVID-19. The creation of a protective vaccine could

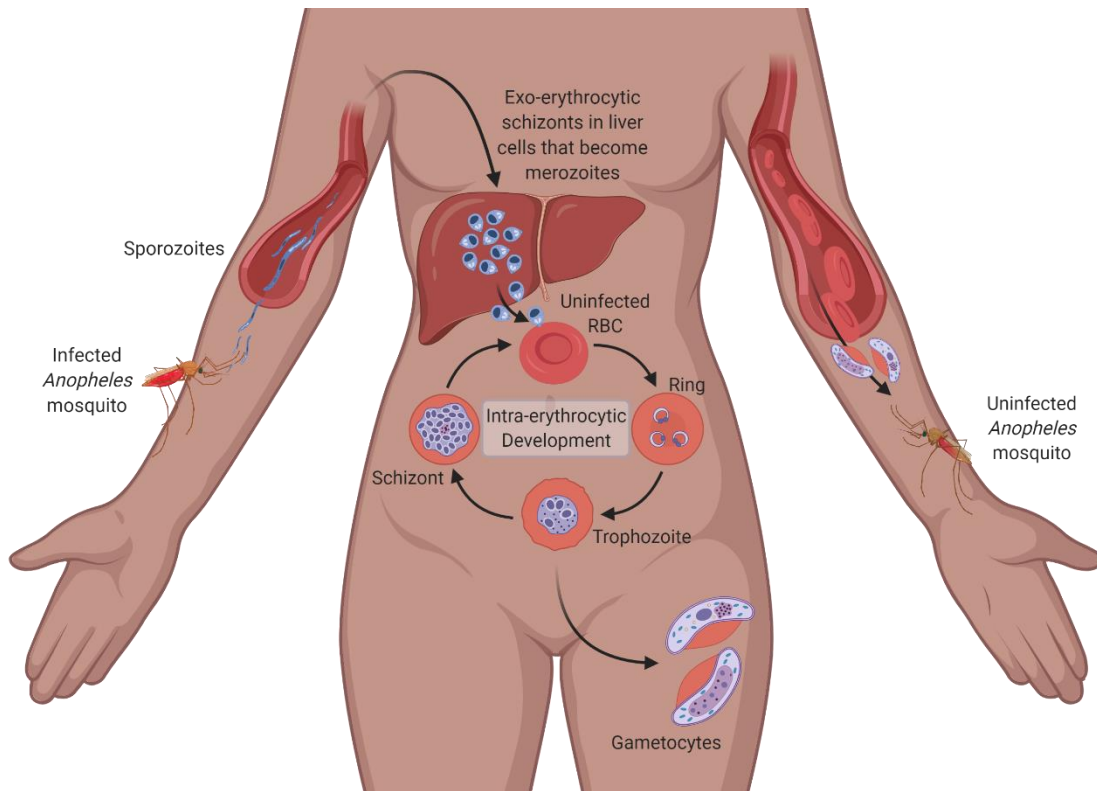
drastically reduce malaria incidence, but the parasites' complex life cycle and biology has made it difficult to design a vaccine that leads to long lasting protection. To imagine other possible vaccine designs, it is important to understand the life cycle of *Plasmodium* species.

### **The Complicated Life of *Plasmodium* Requires Multiple Points of Intervention**




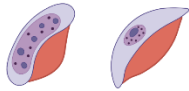

*Plasmodium* is a genus of single-celled parasites that cause malaria. *Plasmodium falciparum* has a vector-host-vector life cycle (seen in **Figure 1**) that starts with an infected female *Anopheles* mosquito. This mosquito injects sporozoites into the bloodstream of an uninfected human host during a blood meal which travel and sequester into hepatocytes. After replicating in the liver, merozoites burst out and re-enter the bloodstream, invade red blood cells (RBCs) and begin an asexual reproduction cycle. Each intra-erythrocytic development cycle (IDC) takes approximately two days as the invading merozoites morph from rings (noted from their ring-like appearance) to trophozoites and finally schizonts that contain roughly 10-fold merozoites inside the RBC. The RBC and parasite membrane undergo proteolysis and the new merozoites invade nearby RBCs and begin the next IDC. Some of these blood stage parasites can differentiate into gametocytes which are able to be taken up a new, uninfected mosquito upon a blood meal. Gametocytes will sexually replicate within the mosquito midgut before being transmitted to another host by the new vector.

A critical feature of *Plasmodium falciparum* is the changing surface proteins as the parasite moves through its life cycle, summarized in **Figure 2**. The surface of the sporozoite parasite plasma membrane (PPM) is decorated with proteins to aid with invasion into the liver<sup>15</sup>. Merozoites have their PPM marked with proteins unique to their internal biology such as rhoptries and the apicoplast that aid in invasion of red blood cells<sup>16</sup>. Blood stage parasites that take on ring, trophozoite and schizont forms inside erythrocytes are surrounded by a secondary membrane, the parasitophorous vacuolar membrane (PVM), which is formed during ingress of the parasite into the RBC. For blood stage parasites, it is this PVM that is decorated with proteins, typically with the purpose of exchanging nutrients with the host cell and remodeling the RBC surface and interior to help evade the immune system<sup>17–21</sup>. As gametocytes arise from differentiated blood stage parasites, they are also surrounded by a PVM and have proteins that are essential for maturation and sexual reproduction within the mosquito midgut<sup>22–26</sup>. Ookinetes and oocysts, the developmental form within the mosquito midgut, only possess a PPM and have surface expression of proteins that are essential for ookinete to oocyst development in the mosquito midgut for the formation of new sporozoites<sup>27–31</sup>.

The complex life cycle, breadth of surface proteins, and presence or lack of a PVM creates issues in developing vaccines. To tackle these challenges, designs have largely been focused on one stage and can range from pieces of essential proteins to whole parasites. The next section discusses attempts toward a protective vaccine.



**Figure 1. A graphical representation of the life cycle of *Plasmodium falciparum*.** The infection stage for a human host begins with an uninfected human serving as a blood meal for an infected *Anopheles* mosquito. Sporozoites from the infected mosquito's salivary glands travel through the skin to the liver where they develop into exo-erythrocytic schizonts that replicate inside hepatocytes. The blood stage begins once the parasites egress from the liver as merozoites and into the circulatory system to begin an asexual intra-erythrocytic development cycle—changing phases from rings to trophozoites to schizonts that will degrade the RBC membrane and explode out for new merozoites to invade nearby RBCs. The transmission stage starts from a few parasites that differentiate from blood stage phases into gametocytes; these gametocytes can be taken up by an uninfected *Anopheles* mosquito during a blood meal where they will replicate in the mosquito midgut before producing sporozoites that will transmit malaria to another human host. Created with BioRender.com.

Phase	Graphic	Example Proteins	PPM	PVM
Sporozoites		Circumsporozoite protein (CSP) BEM46-like protein (PBLP) Thrombospondin-related sporozoite protein (TRSP) Thrombospondin-related anonymous protein (TRAP) Sporozoite surface protein 3 (SSP3)	✓	✗
Merozoites		Merozoite surface proteins (MSPs) Rhoptry proteins (PFRHs) Apical membrane antigen 1 (AMA1) Serine repeat antigens (SERAs)	✓	✗
Rings Trophozoites Schizonts		Early transcribed membrane proteins (eTRAMPs) Exported proteins (EXPs) Rhoptry neck protein 3 (RON3) <i>Plasmodium</i> translocon of exported proteins (PTEX)	✓	✓
Gametocytes		Gametocyte exported proteins (e.g., PfGEXP5, 7, 10) Male gametocyte protein (P230p) Multi-domain adhesion proteins (PfCCps) 6-cys family of proteins (p48/45, p47, p230)	✓	✓
Oocysts		P25 P28 Oocyst capsule protein (PfCap380)	✓	✗

**Figure 2. Graphical table of different forms parasites can take in the human host or mosquito vector.** This graphical table lists example proteins found on the surface of the parasite and whether or not it has just a PPM or a PPM and a PVM. Created with BioRender.com.

## Vaccine Attempts Have Yet to Yield True Protection

Regardless of subunit or whole cell approaches, vaccine attempts against malaria have largely been focused on a single stage: infection (also called pre-erythrocytic), blood, or transmission.

The first malaria vaccine to be recommended for use in children living in highly endemic regions of Africa is the RTS,S vaccine developed by GlaxoSmithKline. RTS,S is comprised of the central NANP repeat region of *Plasmodium falciparum* circumsporozoite protein (CSP) and T-cell epitopes fused to Hepatitis B virus surface antigens that have self-assembled into virus-like particulates<sup>32</sup>. This subunit approach to the infection stage of malaria has made great strides, but the efficacy of the RTS,S vaccine as deployed with adjuvant AS01 leaves something to be desired. In a seven-year study done by Olotu et al covering the efficacy of the RTS,S/AS01 vaccine in African children, they found that efficacy decreases over time, from 35.9% in the first year down to 3.6% by the seventh year<sup>33</sup>. Additionally, there is a large difference in efficacy between vaccinated children living in low exposure areas versus high exposure areas, with high exposure areas having more incidences of malaria than in the control group. This potential for “malaria rebound”, where malaria incidence rebounds to the level it was before any intervention, has been suggested as a possibility after pre-erythrocytic vaccination due to a high amount of antibody titers that protect against sporozoite invasion, but not against blood stage malaria<sup>34</sup>.

Another pre-erythrocytic option that has been studied is whole sporozoites, whether they are irradiated, genetically attenuated, or treated with drugs. Irradiated sporozoites (irrSPZ) have shown to be protective, but only in high titers of intravenously injected irrSPZ ( $1.35 \times 10^5$ ) and high number of doses (5)<sup>35,36</sup> in malaria-naïve participants. When five immunizations of similar titers of irrSPZ ( $2.7 \times 10^5$ )

were given to malaria-exposed adults in Mali, 66% of vaccinated individuals contracted malaria<sup>37</sup> from natural infection despite vaccination. These differences might be due in part to the aforementioned malaria rebound, but also could be due to the high level of transmission in Mali. Thus, there also exists a need to be able to elicit immune responses to the transmission of malaria.

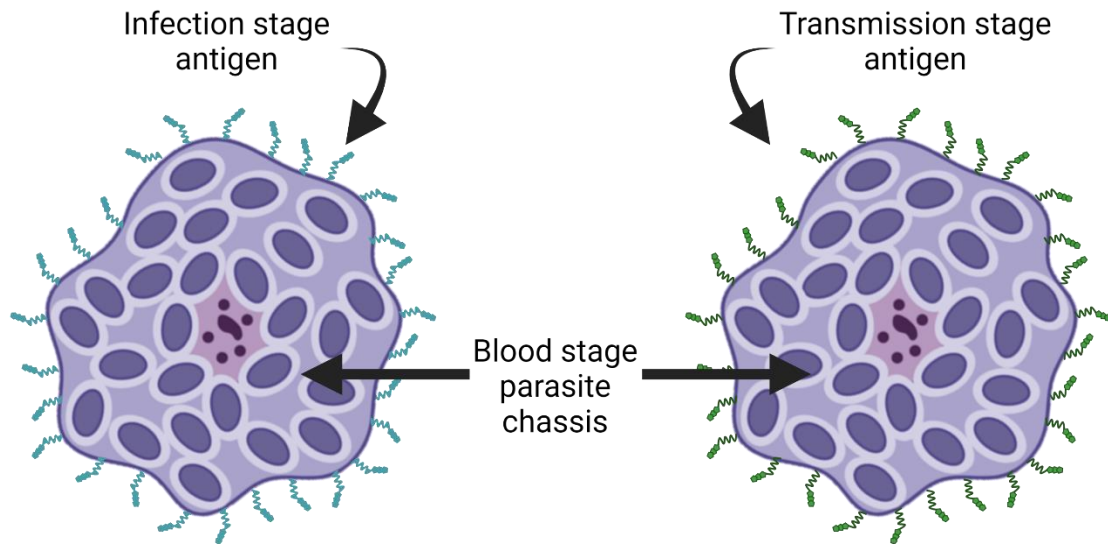
Blood stage malaria vaccines have not come as far as pre-erythrocytic vaccines have, but there has been significant progress in development toward a vaccine. One of the leading blood-stage vaccine candidates utilizes apical membrane antigen 1 (AMA1) and has been tested in a 10-participant group using 3 doses. It demonstrated a dose-response relationship where increasing amounts of antigen resulted in increasing antibody titers by ELISA, with 92% of participants having detectable  $\alpha$ -AMA1 immunoglobulins after the third vaccination<sup>38</sup>. This work has been done in malaria-naïve participants (and small animal testing, such as in rabbits<sup>39</sup>), so only time will tell how this design fares in a malaria-endemic region.

Transmission stage malaria vaccines are few and far between, but the leading ones primarily focus on targeting ookinete surface proteins P25/P28<sup>40</sup>. It is hypothesized that by targeting transmission stage proteins, antibodies against these proteins would be ingested alongside a blood meal into the mosquito where ookinetes could be opsonized and further development into sporozoites would be arrested. While there have been successes in eliciting good antibody titers in mice and in some human trials, there is still work to be done in generating large enough immune responses to be able to produce transmission blocking attempts in challenge models and to account for high transmission settings such as in endemic regions<sup>30,41-43</sup>.

### **Proposal for a New Malaria Vaccine Design**

To address the void of a vaccine design that targets more than one stage of the life cycle and combines the use of subunits and whole cells, I have devised a transgenic parasite concept that utilizes a whole blood stage parasite as a chassis to display key pre-erythrocytic or transmission antigens. **Figure 3** depicts the designs for antigen presentation on an intact blood stage schizont.

Engineered parasites can be isolated from RBC hosts and used to inoculate mice for immunogenicity testing. If humoral responses are generated against the displayed antigens and the native proteins on the whole parasites, then further testing can be done to challenge mice and assess protection and potential correlates of protection. This work aims to design, produce, and characterize transgenic parasites that express antigens outside of their native contexts as well as isolate them from their erythrocyte hosts. Outlining of animal work has also been done to serve as a guide for future work done within this space.



**Figure 3. A graphical representation of the proposed malaria design for this work: EPAPs or engineered parasites for antigen presentation.** As a proof of concept, this design features an intact blood stage parasite acting as a chassis to present an antigen from another stage in the life cycle, either an infection stage antigen or a transmission stage antigen. Created with BioRender.com.

## Chapter I References

1. WHO. *World Malaria Report 2021*. <https://www.who.int/teams/global-malaria-programme/reports/world-malaria-report-2021> (2021).
2. Snow, R. W. & Omumbo, J. A. Chapter 14 - Malaria. in *Disease and mortality in sub-Saharan Africa. 2nd edition* (2010). doi:<http://dx.doi.org/10.1016/B978-0-12-373600-0.00014-7>.
3. Bhatt, S. *et al.* The effect of malaria control on *Plasmodium falciparum* in Africa between 2000 and 2015. *Nature* **526**, 207–211 (2015).
4. Lindsay, S. W., Thomas, M. B. & Kleinschmidt, I. Threats to the effectiveness of insecticide-treated bednets for malaria control: thinking beyond insecticide resistance. *Lancet Glob. Heal.* **9**, e1325–e1331 (2021).
5. Ranson, H. & Lissenden, N. Insecticide Resistance in African *Anopheles* Mosquitoes: A Worsening Situation that Needs Urgent Action to Maintain Malaria Control. *Trends Parasitol.* **32**, 187–196 (2016).
6. Njumkeng, C. *et al.* Coverage and usage of insecticide treated nets (ITNs) within households: Associated factors and effect on the prevalence of malaria parasitemia in the Mount Cameroon area. *BMC Public Health* **19**, 1–11 (2019).
7. Shah, M. P. *et al.* The effectiveness of older insecticide-treated bed nets (ITNs) to prevent malaria infection in an area of moderate pyrethroid resistance: Results from a cohort study in Malawi. *Malar. J.* **19**, 1–12 (2020).
8. Tangena, J. A. A. *et al.* Indoor residual spraying for malaria control in sub-Saharan Africa 1997 to 2017: An adjusted retrospective analysis. *Malar. J.* **19**, 1–15 (2020).
9. Sherrard-Smith, E. *et al.* Systematic review of indoor residual spray efficacy and effectiveness against *Plasmodium falciparum* in Africa. *Nat. Commun.* **2018 91** **9**, 1–13 (2018).
10. WHO. Global Plan for Insecticide Resistance Management. (2012).
11. Dondorp, A. M. *et al.* Artemisinin Resistance in *Plasmodium falciparum* Malaria. *N. Engl. J. Med.* **361**, 455 (2009).
12. Yobi, D. M. *et al.* Assessment of *Plasmodium falciparum* anti-malarial drug resistance markers in *pfk13*-propeller, *pfcr1* and *pfmdr1* genes in isolates from treatment failure patients in Democratic Republic of Congo, 2018–2019. *Malar. J.* **20**, 1–8 (2021).
13. Hussien, M. *et al.* Antimalarial drug resistance molecular markers of *Plasmodium falciparum* isolates from Sudan during 2015–2017. *PLoS One* **15**, e0235401 (2020).
14. White, N. J. Triple artemisinin-containing combination anti-malarial treatments should be implemented now to delay the emergence of resistance. *Malaria Journal* (2019) doi:10.1186/s12936-019-2955-z.
15. Swearingen, K. E. *et al.* Interrogating the *Plasmodium* Sporozoite Surface: Identification of Surface-Exposed Proteins and Demonstration of Glycosylation on CSP and TRAP by Mass Spectrometry-Based Proteomics. *PLoS Pathog.* **12**, (2016).
16. Beeson, J. G. *et al.* Merozoite surface proteins in red blood cell invasion, immunity and vaccines against malaria. *FEMS Microbiol. Rev.* **001**, 343–372 (2016).
17. Beckid, J. R. & Hoid, C.-M. Transport mechanisms at the malaria parasite-host cell interface. (2021) doi:10.1371/journal.ppat.1009394.
18. Mackellar, D. C., Vaughan, A. M., Aly, A. S. I., Deleon, S. & Kappe, S. H. I. A systematic analysis of the early transcribed membrane protein family throughout the life cycle of *Plasmodium yoelii*. *Cell. Microbiol.* (2011) doi:10.1111/j.1462-5822.2011.01656.x.
19. Spielmann, T., Montagna, G. N., Hecht, L. & Matuschewski, K. Molecular make-up of the *Plasmodium* parasitophorous vacuolar membrane. *International Journal of Medical Microbiology* (2012) doi:10.1016/j.ijmm.2012.07.011.
20. Nessel, T. *et al.* EXP1 is required for organization of the intraerythrocytic malaria parasite vacuole.

- bioRxiv* (2019) doi:10.1101/752634.
21. Mesén-Ramírez, P. *et al.* EXP1 is critical for nutrient uptake across the parasitophorous vacuole membrane of malaria parasites. *PLOS Biol.* (2019) doi:10.1371/journal.pbio.3000473.
  22. Tibúrcio, M. *et al.* Specific expression and export of the *Plasmodium falciparum* Gametocyte Exported Protein-5 marks the gametocyte ring stage. *Malar. J.* **14**, 1–12 (2015).
  23. Marin-Mogollon, C. *et al.* The *Plasmodium falciparum* male gametocyte protein P230p, a paralog of P230, is vital for ookinete formation and mosquito transmission. *Sci. Reports 2018 81* **8**, 1–13 (2018).
  24. Messina, V. *et al.* Gametocytes of the malaria parasite *Plasmodium falciparum* interact with and stimulate bone marrow mesenchymal cells to secrete angiogenetic factors. *Front. Cell. Infect. Microbiol.* **8**, 50 (2018).
  25. Scholz, S. M. *et al.* PfCCp proteins of *Plasmodium falciparum*: gametocyte-specific expression and role in complement-mediated inhibition of exflagellation. *Int. J. Parasitol.* **38**, 327–340 (2008).
  26. van Dijk, M. R. *et al.* Three Members of the 6-cys Protein Family of *Plasmodium* Play a Role in Gamete Fertility. *PLOS Pathog.* **6**, e1000853 (2010).
  27. Sharma, B. & Jaiswal, M. K. The P25 Ookinete Surface Proteins: Homology Modeling and Phylogenetic Relationships. *ISRN Comput. Biol.* (2013) doi:10.1155/2013/391018.
  28. Saxena, A. K. *et al.* The essential mosquito-stage P25 and P28 proteins from *Plasmodium* form tile-like triangular prisms. *Nat. Struct. Mol. Biol.* (2006) doi:10.1038/nsmb1024.
  29. Baton, L. A. & Ranford-Cartwright, L. C. Do malaria ookinete surface proteins P25 and P28 mediate parasite entry into mosquito midgut epithelial cells? *Malaria Journal* (2005) doi:10.1186/1475-2875-4-15.
  30. Saxena, A. K., Wu, Y. & Garboczi, D. N. *Plasmodium* P25 and P28 surface proteins: Potential transmission-blocking vaccines. *Eukaryotic Cell* (2007) doi:10.1128/EC.00060-07.
  31. Itsara, L. S. *et al.* PfCap380 as a marker for *Plasmodium falciparum* oocyst development in vivo and in vitro. *Malar. J.* **17**, 1–13 (2018).
  32. Kaslow, D. C. & Biernaux, S. RTS, S: Toward a first landmark on the Malaria Vaccine Technology Roadmap. *Vaccine* (2015) doi:10.1016/j.vaccine.2015.09.061.
  33. Bejon, P. *et al.* Efficacy of RTS,S/AS01E vaccine against malaria in children 5 to 17 months of age. *N. Engl. J. Med.* (2008) doi:10.1056/NEJMoa0807381.
  34. Bejon, P. *et al.* Effect of the Pre-erythrocytic Candidate Malaria Vaccine RTS,S/AS01E on Blood Stage Immunity in Young Children. *J. Infect. Dis.* **204**, 9–18 (2011).
  35. Seder, R. A. *et al.* Protection Against Malaria by Intravenous Immunization with a Nonreplicating Sporozoite Vaccine. *Science (80-. )*. **341**, 1359–1365 (2013).
  36. Goh, Y. S., McGuire, D. & Rénia, L. Vaccination with sporozoites: Models and correlates of protection. *Frontiers in Immunology* (2019) doi:10.3389/fimmu.2019.01227.
  37. Sissoko, M. S. *et al.* Safety and efficacy of PfSPZ Vaccine against *Plasmodium falciparum* via direct venous inoculation in healthy malaria-exposed adults in Mali: a randomised, double-blind phase 1 trial. *Lancet Infect. Dis.* **17**, 498–509 (2017).
  38. Malkin, E. M. *et al.* Phase 1 clinical trial of apical membrane antigen 1: An asexual blood-stage vaccine for *Plasmodium falciparum* malaria. *Infect. Immun.* **73**, 3677–3685 (2005).
  39. Kocken, C. H. M. *et al.* High-level expression of the malaria blood-stage vaccine candidate *Plasmodium falciparum* apical membrane antigen 1 and induction of antibodies that inhibit erythrocyte invasion. *Infect. Immun.* **70**, 4471–4476 (2002).
  40. Chaturvedi, N., Bharti, P. K., Tiwari, A. & Singh, N. Strategies & recent development of transmission-blocking vaccines against *Plasmodium falciparum*. *Indian J. Med. Res.* **143**, 696 (2016).
  41. Kapulu, M. C. *et al.* Comparative Assessment of Transmission-Blocking Vaccine Candidates against *Plasmodium falciparum*. *Sci. Reports 2015 51* **5**, 1–15 (2015).



42. Miura, K. *et al.* Functional comparison of plasmodium falciparum transmission-blocking vaccine candidates by the standard membrane-feeding assay. *Infect. Immun.* **81**, 4377–4382 (2013).
43. Takashima, E. *et al.* Identification of Novel Malaria Transmission-Blocking Vaccine Candidates. *Front. Cell. Infect. Microbiol.* **11**, 1224 (2021).

## Chapter II: Expressing Antigens outside their Native Contexts

### Abstract

There is a void in malaria vaccine designs for a single injectable that covers multiple stages of the parasite life cycle. To address this, we designed plasmids and generated transgenic parasite lines that utilize a blood stage parasite as a scaffold to present non-blood stage antigens. A protein native to the parasitophorous vacuolar membrane, eTRAMP4, was fused to either the pre-erythrocytic stage circumsporozoite protein or the transmission stage protein P25. This proof-of-concept design was then assessed using a *Renilla* luciferase growth assay, Western blots, and immunofluorescence assays. We determined that protein fusions do not inhibit parasite growth, are the correct length appropriate for the fusions, and localize to the parasitophorous vacuolar membrane.

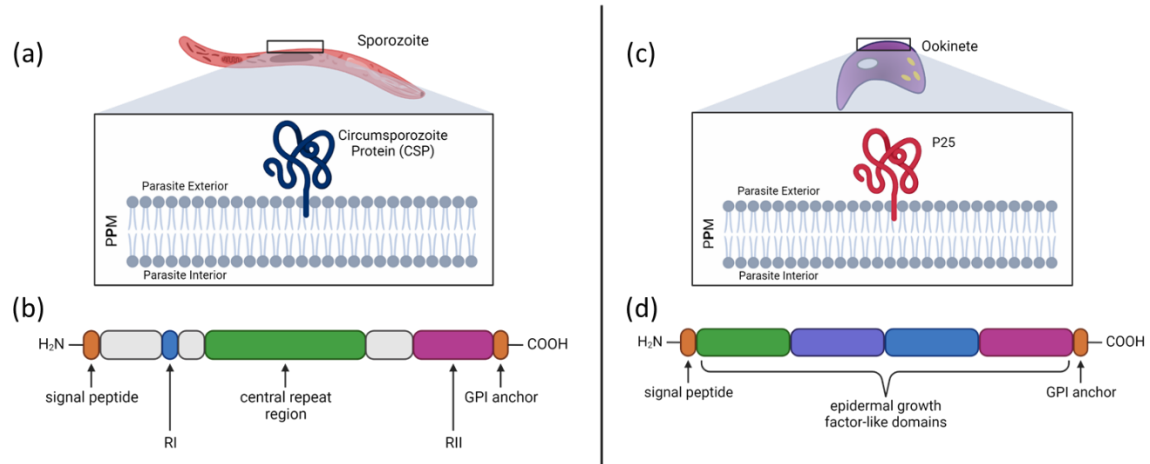
### Introduction

As mentioned in the previous chapter, “malaria rebound” has been suggested as a possibility after pre-erythrocytic vaccination, due to high antibody titers that protect against sporozoite invasion but not blood stage malaria. This work aims to address the void in vaccine designs and create a proof-of-concept for a single injectable that could elicit protection against multiple stages. To this end, we have envisioned a blood stage parasite that ectopically expresses native antigens outside of their native contexts. These antigens would be either from the pre-erythrocytic or transmission stage of malaria and combined with the blood stage chassis are hypothesized to cover pre-erythrocytic-and-blood stages or blood-and-transmission stages. For these antigens, we have chosen two well-known and well-characterized proteins: circumsporozoite protein (CSP) from the pre-erythrocytic stage and protein 25 (P25) from the transmission stage.

Circumsporozoite protein (CSP) is a highly conserved protein that forms a dense coat on the surface of sporozoites and is critical for their invasion into hepatocytes (Figure 4, (a)). CSP is comprised of a central repeat region flanked by two conserved domains—a C-terminal sequence akin to a type I thrombospondin repeat and an N-terminal 5 amino acid sequence simply known as region I<sup>1</sup> (Figure 4, (b)). In addition to these domains, CSP also contains a glycosylphosphatidylinositol (GPI) sequence on its C terminus that serves to anchor the protein in the exterior leaflet of the parasite plasma membrane (PPM). CSP is a well-known vaccine candidate<sup>2,3</sup>, most notably being the antigen for the RTS,S vaccine that has received official endorsement by the WHO in October 2021 for use in endemic African regions<sup>4</sup>. With CSP being the most abundant protein on the sporozoite surface<sup>5</sup>, it is a prime protein to serve as an antigen in our envisioned design. By targeting CSP, this work aims to stop the initial infection into hepatocytes, preventing a patient from contracting malaria and proceeding to the asexual blood stage, as others have done using antibodies against CSP<sup>6</sup>.

Surface protein P25 (or P25) is another highly conserved protein that is prominently displayed on the ookinete plasma membrane as it resides in the mosquito midgut (Figure 4, (c)). This protein has an N-terminal signal peptide, followed by four epidermal growth factor (EGF)-like domains and a C-terminal GPI anchor<sup>7</sup> (Figure 4, (d)). P25 is hypothesized to be involved in cell-to-cell or cell-to-peritrophic

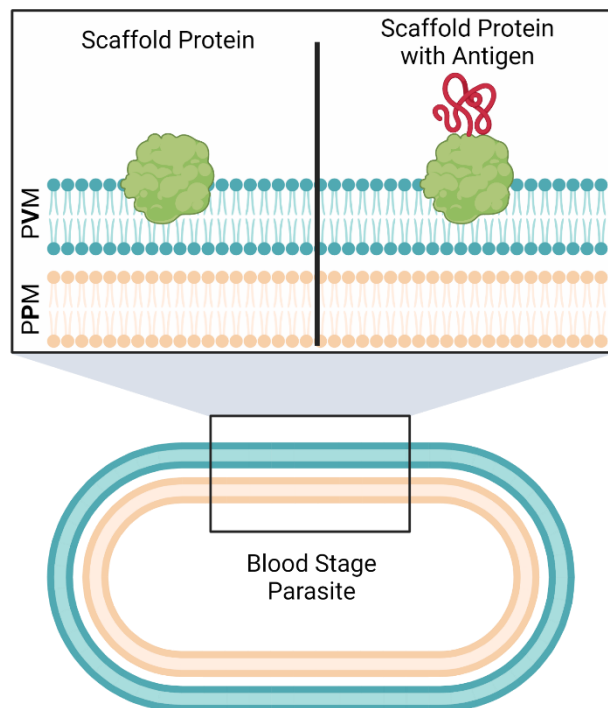
matrix interactions that allow for ookinete motility into mosquito epithelial cells for oocyst formation<sup>8,9</sup>. By targeting P25, this work aims to block transmission of parasites to humans through the inhibitory action of host-produced anti-P25 antibodies in the mosquito blood meal on parasite sexual reproduction within the mosquito midgut, as others have observed in various studies<sup>8</sup>.



**Figure 4. A graphical representation of the two antigens for the proof-of-concept: CSP (left) and P25 (right).** (a) A representation of a sporozoite that shows the orientation of the circumsporozoite protein in the exterior leaflet of the parasite plasma membrane (PPM). (b) A representation of the wild type CSP sequence that features (from N terminus to C terminus) a signal peptide, Region I (RI), a central repeat region, Region II (RII), and a GPI anchor that anchors the protein into the PPM. (c) A representation of an ookinete that shows the orientation of the P25 in the exterior leaflet of the parasite plasma membrane (PPM). (d) A representation of the wild type P25 sequence that features (from N terminus to C terminus) a signal peptide, four epidermal growth factor-like domains (EGFLs), and a GPI anchor that anchors the protein into the PPM. Created with BioRender.com.

While CSP and P25 are presented on the PPM via GPI anchor, the envisioned chassis for these antigens—a blood stage parasite—has an extra membrane that encapsulates the PPM: the parasitophorous vacuolar membrane, as can be seen in Figure 5. To present antigens on the surface of this blood stage parasite, we aim to use a protein native to the PVM (Figure 5, inset left) to fuse our antigens of interest onto so they are displayed on the exterior of the parasite (Figure 5, inset right). By removing the GPI anchor from CSP and P25, we can instead fuse these antigens to a PVM-localized protein on a blood stage parasite for presentation and create a single-bodied injectable that could provide protection for multiple stages of malaria.

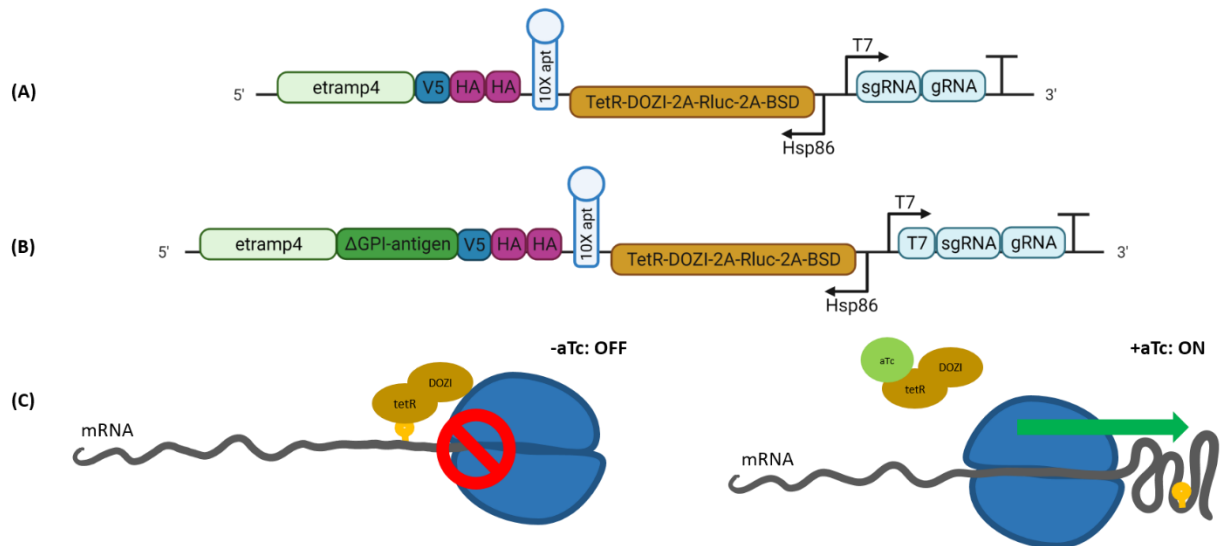
For the scaffold protein we have chosen to use one of the early transcribed membrane proteins, eTRAMP4. eTRAMP4 is highly conserved across *Plasmodium* species and is expressed during every form of the blood stage on the PVM, with high peaks in expression during rings and schizonts<sup>10</sup>. Additionally, eTRAMP4 is also non-essential, which is ideal for ensuring that protein fusion will not result in defects to parasite growth. For these reasons, eTRAMP4 is a good candidate for scaffold usage.



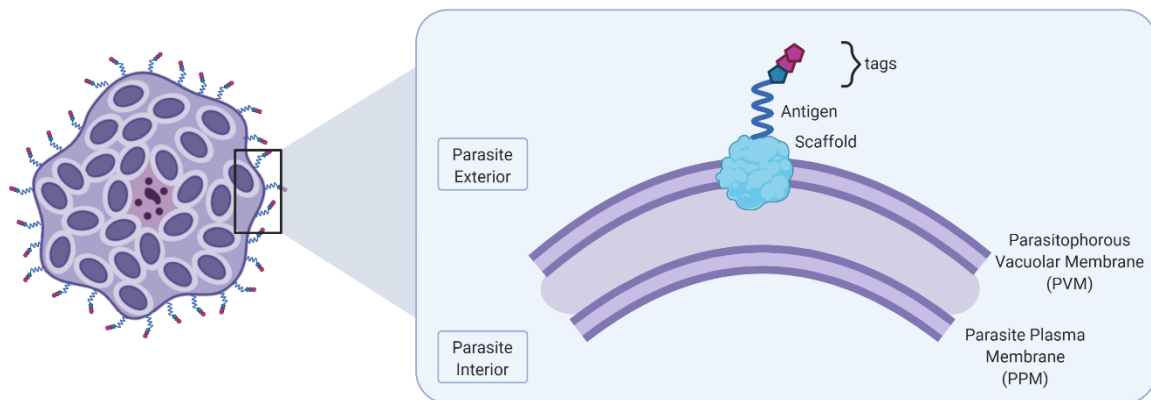
**Figure 5. Graphical representation of blood stage parasite membranes and the scaffold protein.** The scaffold protein natively sits in the outer leaflet of the PVM (inset left) while the transgenic parasites would express a fused antigen to this scaffold (inset right). The PVM surrounds the PPM for blood stage parasites. Created with BioRender.com.

In this work, plasmids have been generated with the TetR-DOZI translational repressor system which allows for conditional expression within transfected parasites based on the absence or presence of anhydrous tetracycline (aTc). In the absence of aTc, the repressor TetR-DOZI binds to the aptamer array and blocks translation of mRNA. In the presence of aTc, aTc allosterically binds to TetR-DOZI and a conformational change causes TetR-DOZI to detach from the aptamer array and allowing translation to proceed. A summary of this conditional system can be seen in **Figure 6**, with (a) showing the eTRAMP4 scaffold plasmid design alone, (b) showing the protein fusion plasmid design, and (c) showing the conditional expression with aTc. We will be utilizing this conditional expression for characterizing our transgenic parasite lines.

For this proof-of-concept, this chapter focuses on the plasmid generation and characterizing the subsequent transgenic parasites. This characterization process has been done using growth assays to determine that antigen fusion does not harm parasite growth; Western blots to determine that the appropriate protein length is achieved that corresponds to fusion of the scaffold protein eTRAMP4 to the antigens CSP and P25; and immunofluorescence assays and determine if the fused antigens localize to the PVM instead of the native context PPM. Our final envisioned design can be seen in **Figure 7**, with a blood stage schizont that expresses scaffold protein fused to antigen with accompanying characterization tags on the exterior of the PVM.



**Figure 6. Vector design and translational repressor system.** Vector designs for (A) protein scaffold and the (B) protein fusion utilize the pSN054 backbone. (C) The translational repressor system with TetR-DOZI in the absence and presence of an analog to tetracycline, aTc, is used to conditionally express proteins in transgenic parasite lines. (A) and (B) created with BioRender.com.



**Figure 7. Imagined design of presenting antigens on scaffold protein on the blood stage parasite surface.** Created with BioRender.com.

## Methods

### Plasmid Vector Design

The plasmid vectors were designed on a pSN054 backbone<sup>11</sup> which contains V5, HA, myc, and FLAG tags; a 10X aptamer array; 3' UTR; a TetR-DOZI cassette with Blasticidin resistance, *Renilla* luciferase (Rluc), and a Hsp86 promoter; as well as a T7 promoter with guide RNA (gRNA) for CRISPR editing in parasites. eTRAMP4 left and right homology regions (LHR and RHR) was generated via PCR using the appropriate primers as listed in the below table. The recoded region sequence was generated using NetPremier from Premier Biosoft and is included below for reference. Both the recoded region and the guide RNA (sgRNA) were ordered as tiles from Codex and synthesized on the BioXp system. The pSN054 backbone was restriction digested with I-Sce1 and the RHR was added using Gibson Assembly

(Gibson Assembly Ultra Kit from VWR). TSA BigEasy Electrocompetent *E. coli* cells (VWR) were transformed and successful colonies were mini-prepped using the NucleoSpin Plasmid mini-prep kit (Takara). The pSN054+RHR was restriction digested using FseI and AsiSI and the LHR and recoded regions were inserted using Gibson Assembly. This assembly was transformed into TSA BigEasy cells and mini-prepped, with confirmation of lengths done using gel electrophoresis. PCR was done using the below primers for CSP and P25 without their GPI anchors ( $\Delta$ GPI-CSP and  $\Delta$ GPI-P25). The fully assembled eTRAMP4 construct was digested with AsiSI and  $\Delta$ GPI-CSP and  $\Delta$ GPI-P25 were inserted into their own eTRAMP4 construct using Gibson Assembly. These two constructs were checked for appropriate length using gel electrophoresis after mini-prepping. Maxi-preps (Nucleobond Xtra Midi Kit for Maxipreps from Takara) were performed for all three constructs and an aptamer check was done by digesting the maxi-preps using XmaI and running on a gel. Maxi-prepped plasmids could then be used in transfections to create parasite lines.

**Table 1. List of plasmid assembly sequences for the eTRAMP4 scaffold and the two antigens, CSP and P25.**

<b>eTRAMP4 (Pf3D7_0423700) Scaffold into pSN054 Backbone</b>	
LHR forward primer	atgcataccgaaaaacatagaatatttaaa
LHR reverse primer	cctttattttttttttctcacccaagcaaaaaATGAAGCTTTCAAAT
Recoded region	ATGAAGCTTTCAAATCTTTTCTATGTGTTTCGCATTGTTGATATCAATGAATGTGT TTGTGCCTGGTTTCATGAATGTTCTTGGTAAGAACGTGAACGTGGACTCAATCG TGATGTCAAAGATAGATGAAATGCAGAAAAAGAAGCAGCAGCAGAAGATCAT CATGATCAGCACGGTGGTGACGGGGTTGGCACTTTTGCTTGGGTCAGCACTTG GGTTCGGGTACTTGTCAAAGAGCAACAAGAAGCCTGAGGTTAGCGGGGATGA GAAGGACGAGTCAAAGAAGGTTGACGCTGGTAAGAACAATAAGGAGAGTAA GGCAGACAAGAGCGAGGAGAAGCTTCATAAGAGCGACGACCGTGAGTCAAA GAGCAGCAGCAGCAAGAGCACCGCTGTTCCAACGACGGTG
RHR forward primer	tgcatagtcttgagatcgtagt
RHR reverse primer	tgagattacatgaggacacaca
sgRNA	ATGATATCTACTGTTGTTAC
<b>CSP (Pf3D7_0304500) without GPI Anchor (<math>\Delta</math>GPI-CSP)</b>	
Forward primer	AAGAGCACCGCTGTTCCAACGACGGTGgcatcgcgTTATTCCAGGAATACCACT GCTATGGAAG
Reverse primer	GAGGAGAGGGTTAGGGATAGGCTTACCgcatcgcgATTACGACATTAAACACA CTGGAAC
<b>P25 (Pf3D7_1030900) without GPI Anchor (<math>\Delta</math>GPI-P25)</b>	
Forward primer	AAGAGCACCGCTGTTCCAACGACGGTGgcatcgcgGTTACCGTGGATACTGTAT GCAAAAGAGGA
Reverse primer	GAGGAGAGGGTTAGGGATAGGCTTACCgcatcgcgAAAAGCAGTACATATAGA GCTTTCATT

### Parasite Culturing and Transfection

*P. falciparum* parasites from the pCRISPR line (parental line NF54attB<sup>12</sup>, pCRISPR line created in lab by Jeff Wagner to serve as a platform for genome engineering<sup>11</sup>) were grown at 37°C under 5% O<sub>2</sub> and 5% CO<sub>2</sub> in RPMI-1640 media supplemented with 5g/L Albumax II (Life Technologies), 2g/L sodium bicarbonate, 25mM HEPES pH 7.4, 1mM hypoxanthine and 50mg/L gentamicin; this media will be

referred to hereafter as RPMI-C. Human blood from a commercial supplier was used for parasite culture (Research Blood Components, Watertown, MA). Fully transfected parasite lines were cultured using RPMI-C with 500nM anhydrous tetracycline (aTc, Sigma Aldrich) and 2.5µg/mL Blastcidin (RPI Corp). For ease of reference, this will be denoted as +aTc media in this work.

Transfections were performed using a previously described red blood cell pre-loading method<sup>13</sup>. 50-100µg of purified plasmid DNA was mixed with human red blood cells in 0.2cm cuvettes and electroporated with 8 square waves of 365V for 1ms each, separated by 0.1s. The DNA-preloaded RBCs were inoculated with schizont-stage pCRISPR parasites to achieve parasitemias of approximately 1% in +aTc RPMI-C media. Media was changed every day for the first 4 days. Starting 4 days post-transfection, cultures were selected using 2.5µg/mL Blastcidin. Transfection progress was monitored via Giemsa-stained smears (methodology listed in Chapter 3) and *Renilla* luciferase measurements using a 20/20 luminometer as described below.

#### **Renilla Luciferase-Based Growth Assay**

Two days prior to setting up the assay, parasites were sorbitol synchronized using previously described methods<sup>14</sup>. On the day of the assay, parasites were assessed by smearing to ensure they were are ring stage. Cultures were pelleted in 15mL conical tubes, transferred to microcentrifuge tubes, and washed 3 times with warmed RPMI-C media. Cultures were then split to grow in 10mL cultures at 0.1% starting parasitemia and 2% hematocrit, both in +aTc and -aTc conditions, for 96 hours. At IDC 0, 2, and 4, 100µL of culture was put into a 96-well plate with n = 6 for each condition, taking care to avoid the edges for any potential edge effects. The parasite plate for IDC 0 was pelleted down, the media was aspirated, and the plate was foil-wrapped and frozen at -80°C. After their respective IDCs, each plate was pelleted down, media aspirated, and plate frozen until all plates were ready to be measured. To each well, 25µL of 1X Passive Lysis Buffer (PLB) was added and mixed well, followed by 25µL of 1:1 PLB:*Renilla* Luciferase Buffer + Substrate (100:1 buffer:substrate, from Promega Renilla-Glo Luciferase Assay System for Rluc). All plates were measured together on a Promega GloMax Explorer Multimode Microplate Reader.

#### **Western Blotting**

Parasite cultures were transferred into a 15mL conical tube and saponin was added to render a final concentration of 0.0015% saponin. The tubes were then gently inverted several times until cultures became translucent, and then tubes were spun at 3500RPM for 4 minutes. The supernatants were aspirated and the pellets were resuspended in 1mL of 1X PBS before being transferred to microcentrifuge tubes which were then spun at top speed for 1 minute and the PBS aspirated. Pellets were washed 2 more times using this washing method with PBS. The final pellets were then aspirated of PBS. Parasite pellets were resuspended in 100µL of parasite lysis buffer (4mL of 10% sodium dodecyl sulfate SDS, 0.5mL of 10% Triton X-114, 5mL 1X PBS, 0.5mL sterile water) and placed into a 100°C heat block for 2 to 5 minutes. Samples were then spun at top speed for 1 minute to pellet cells. 35µL of parasite lysate was mixed with 7µL of protein loading buffer (SDS and dithiothreitol) and loaded onto Mini-PROTEAN TGX Precast Gels (4-15% gradient from BioRad) in Tris-Glycine buffer. Gels were run at 200V for 30 minutes. After separation by polyacrylamine gel electrophoresis (PAGE),

proteins were transferred to a polyvinylidene fluoride (PVDF) membrane using the Mini Trans-Blot Electrophoretic Transfer Cell system (from BioRad) per manufacturer's instructions and blocked with 10mL of blotto blocking solution (100mg/mL skim milk in 1X TBS/Tween) for 1 hour at room temperature while rocking. Membranes were then placed in 10mL of primary antibody solutions made up in blotto (mouse  $\alpha$ -HA antibody from Cell Signaling Technology, diluted at 1:3000) and rocked overnight at 4°C. Primary antibody solution was triple washed off membranes by dumping out the primary antibody solution, placing the membrane in 10mL of 1X TBS/Tween and rocking for 15 minutes, and dumping out the TBS/Tween wash. A secondary antibody solution was made in blotto ( $\alpha$ -mouse HRP conjugate antibody from Millipore Sigma at 1:3000 dilution). Membranes were incubated in foil-wrapped boxes with secondary antibody solution and rocked at room temperature for 1 hour. Membranes were then washed 3 times using above steps. After a 3-5 minute incubation at room temperature in SuperSignal West Pico Chemiluminescent substrate (ThermoFisher Scientific), protein blots were imaged using the ChemiDoc MP System.

### **Immunofluorescence Assays**

Parasites were centrifuged and culture media was aspirated. Parasites were then washed 3 times with wash media and resuspended in 250 $\mu$ L wash media. A 10 $\mu$ M working stock of MitoTracker (MitoTracker Deep Red FM from ThermoFisher Scientific) was made using RPMI-C and 2.5 $\mu$ L of this working stock was added to the parasites to reach a final concentration of 100nM. Parasites were incubated at 37°C for 15 minutes and washed 2 times with 1mL of wash media at 500g for 1 minute. Parasites were then pelleted and media was aspirated. Each parasite pellet was resuspended in 500 $\mu$ L of fixing solution (4% v/v paraformaldehyde and 0.0075% v/v glutaraldehyde in 1X PBS) and rocked at room temperature for 30 minutes. Parasites were pelleted at 8000 g and washed with 1mL of 1x PBS before being resuspended in 500 $\mu$ L permeabilization solution (0.1% v/v Triton X-100 in 1X PBS) and rocked at room temperature for 10 minutes. Parasites were pelleted at 8000 g and washed with 1mL of 1X PBS. Pellets were then resuspended in 500 $\mu$ L of blocking solution (3% w/v bovine serum albumin in 1X PBS) and rocked at room temperature for 30 minutes. Parasites were pelleted and blocking solution was aspirated before pellets were incubated in 400 $\mu$ L of primary antibody solution (mouse  $\alpha$ -HA primary antibody from Cell Signaling Technology at 1:350 dilution in blocking solution) and rocked overnight at 4°C. Parasites were pelleted and primary antibody solution was aspirated before pellets were incubated in 400 $\mu$ L of secondary antibody solution (Alex Fluor 488-conjugated  $\alpha$ -mouse secondary antibody from Cell Signaling Technology at 1:400 dilution in blocking solution) and rocked for 1 hour at room temperature while protected from light. Parasites were then pelleted and washed in 1X PBS with DAPI (1:1000 DAPI in 1X PBS), rocked for 5 minutes wrapped in foil at room temperature before final pellet and resuspension in 20 to 40 $\mu$ L of 1X PBS. 4 $\mu$ L of sample was transferred onto a slide and dried at 37°C for 10 minutes. 5 $\mu$ L of ProLong Diamond Gold (ProLong Diamond Antifade Mountant from ThermoFisher Scientific) was added to sample, a cover slip was placed, and the slide was dried overnight at 37°C. Final slides were then viewed and imaged using the DeltaVision Elite Widefield Deconvolution imaging system at the W.M. Keck Biological Imaging Facility in the Whitehead Institute.

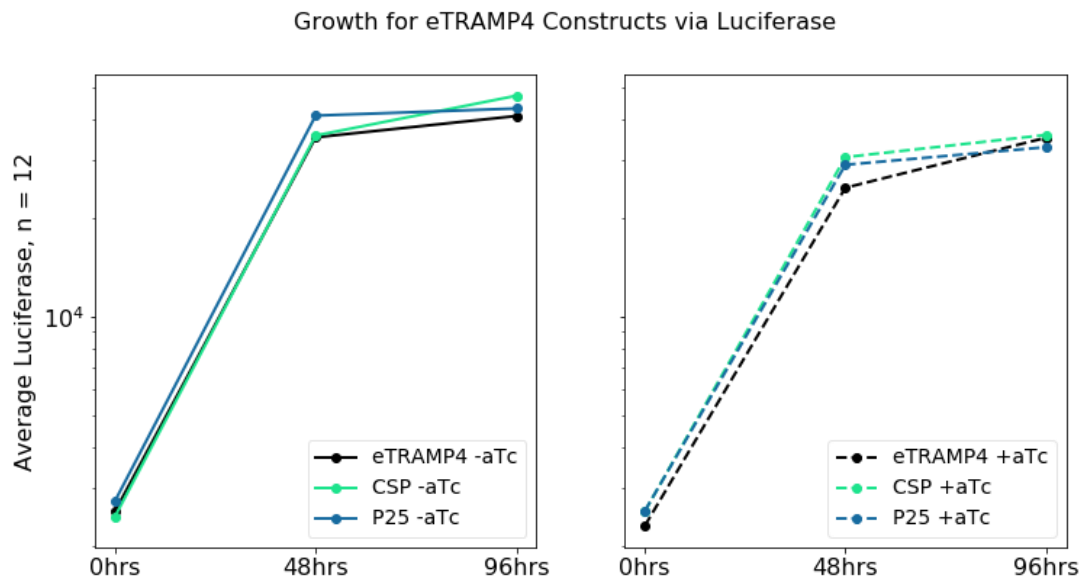


## Results and Discussion

### Fusing Antigens to Scaffold Does Not Affect Parasite Growth

Previous literature has determined that eTRAMP4 knockouts resulted in no change in blood stage parasite growth and thus are nonessential<sup>15</sup>. To confirm that protein fusions do not hinder parasite growth compared to scaffold alone, a growth assay was conducted according to the *Renilla* Luciferase-Based Growth Assay sections in Methods.

**Figure 8** plots the average luciferase ( $n = 12$ ) of the 3 parasite lines, with and without aTc, across 2 IDCs or 96 hours. As the eTRAMP4 scaffold alone is closest to the parasites' native disposition in the blood stage, it serves as a control to compare the growth of protein fusions to. Independent t-tests were used to compare samples. Without aTc (**Figure 8**, left) eTRAMP4-CSP and eTRAMP4 had statistically similar *Renilla* luciferase (Rluc) values that diverged over time ( $p = 0.46, 0.68, 1.21 \times 10^{-7}$  for IDC0, 1, and 2 respectively). A similar effect could be seen in eTRAMP4-P25 ( $p = 0.06, 4.29 \times 10^{-6}, 0.015$ ). Since these parasites are *not* actually expressing the scaffold or fusions, these differences in population can be attributed to noise or starting culture differences that exploded by IDC2. With the addition of aTc (**Figure 8**, right), eTRAMP4-CSP and eTRAMP4 ( $p = 0.04, 6.95 \times 10^{-6}, 0.43$ ) see a dissimilarity that began at IDC0 but closes at IDC2 and this pattern holds for P25 and eTRAMP4 ( $p = 0.02, 1.27 \times 10^{-3}, 0.11$ ). Even though these values are "statistically different" with a cutoff of 0.05 to reject the null hypothesis, the values for eTRAMP4-CSP and -P25 are actually *greater* than the eTRAMP4 alone. Thus, parasites expressing eTRAMP4-CSP and -P25 fusion proteins do not exhibit decreased fitness relative to the eTRAMP4 line, both in the presence and absence of aTc. These data indicate that genetic fusions to eTRAMP4 can be tolerated without parasite viability loss.

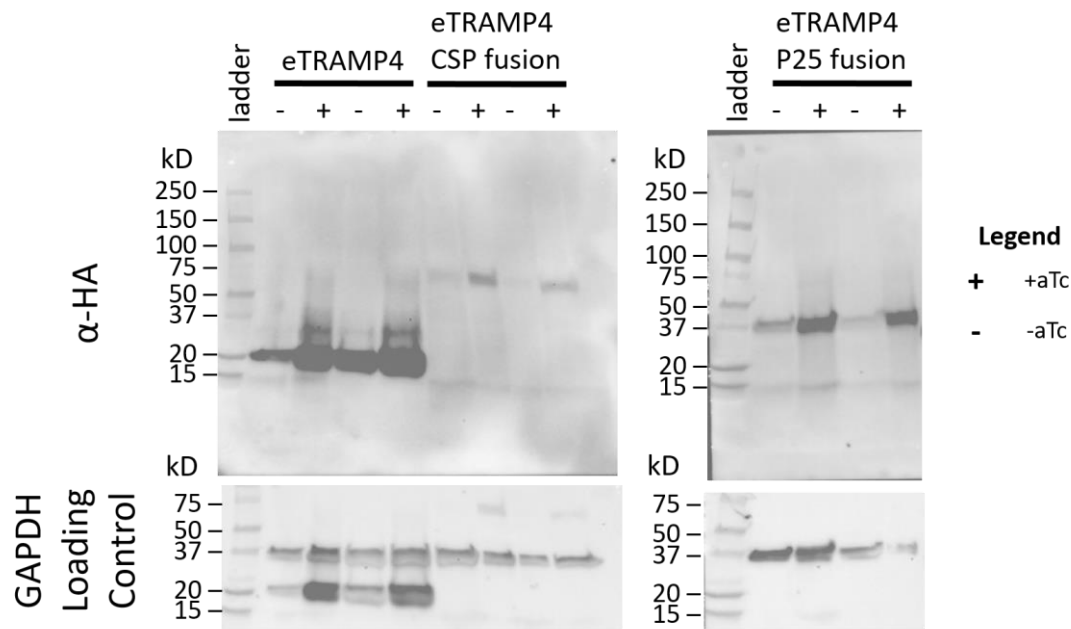


**Figure 8. Parasite growth without aTc (left) and with aTc (right) as measured via luminescence over 96 hours (2 IDCs) for eTRAMP4 constructs.** The eTRAMP4 scaffold alone is depicted in black, protein fusion with CSP in green, and protein fusion with P25 in blue.

### Confirmation of eTRAMP4-CSP and eTRAMP4-P25 fusion protein expression

Western blot analyses were used to confirm fusion protein expression. Previous studies of eTRAMP4 determined that the molecular weight (MW) is approximately 17kD<sup>16</sup>. Further work examined recombinant, full-length CSP and determined its MW to be 55kD<sup>17</sup> while P25 has been noted to run at 25kD<sup>18,19</sup>. **Figure 9** shows immunoblots of the scaffold and the two fusions. Based on in-lab experiments, the MW of the eTRAMP4 construct is approximately 20 kDa. Protein fusions showed an increase in MW, shifting from 20 kDa to 75 kDa for eTRAMP4-CSP and from 20 kDa to more than 37 kDa for eTRAMP4-P25.

As these Western blots were done using parasites grown in the absence or presence of aTc, we can assess the conditional protein expression of our system. Comparing eTRAMP4 -aTc to +aTc, we can see that although there is a large increase in the amount of protein at 20kD, there is not a complete depletion of protein expression as we would otherwise expect for the -aTc condition. This could be due to some leakiness in the TetR-DOZI repressor, as has been noted in previous work<sup>11</sup>. This effect can be seen in both eTRAMP4-CSP and eTRAMP4-P25, though to a lesser degree. From these data, we conclude that we have successfully generated transgenic parasite lines expressing antigens of the expected molecular size and that we can control protein expression using our conditional expression system with TetR-DOZI and the use of aTc.



**Figure 9. Western blots for eTRAMP4 constructs using an HA tag without (-) and with (+) aTc present in culture media.** The top row of images corresponds to those probed for the HA tag at the end of the scaffold or fusion (α-HA) and the bottom row corresponds to α-GAPDH, which is a loading control and runs at approx. 36kD. The scaffold alone runs at approx. 20kD, the fusion with CSP runs at approx. 75kD, and the fusion with P25 runs at approx. 37kD.

### **eTRAMP4-CSP localizes to the parasitophorous vacuolar membrane (PVM)**

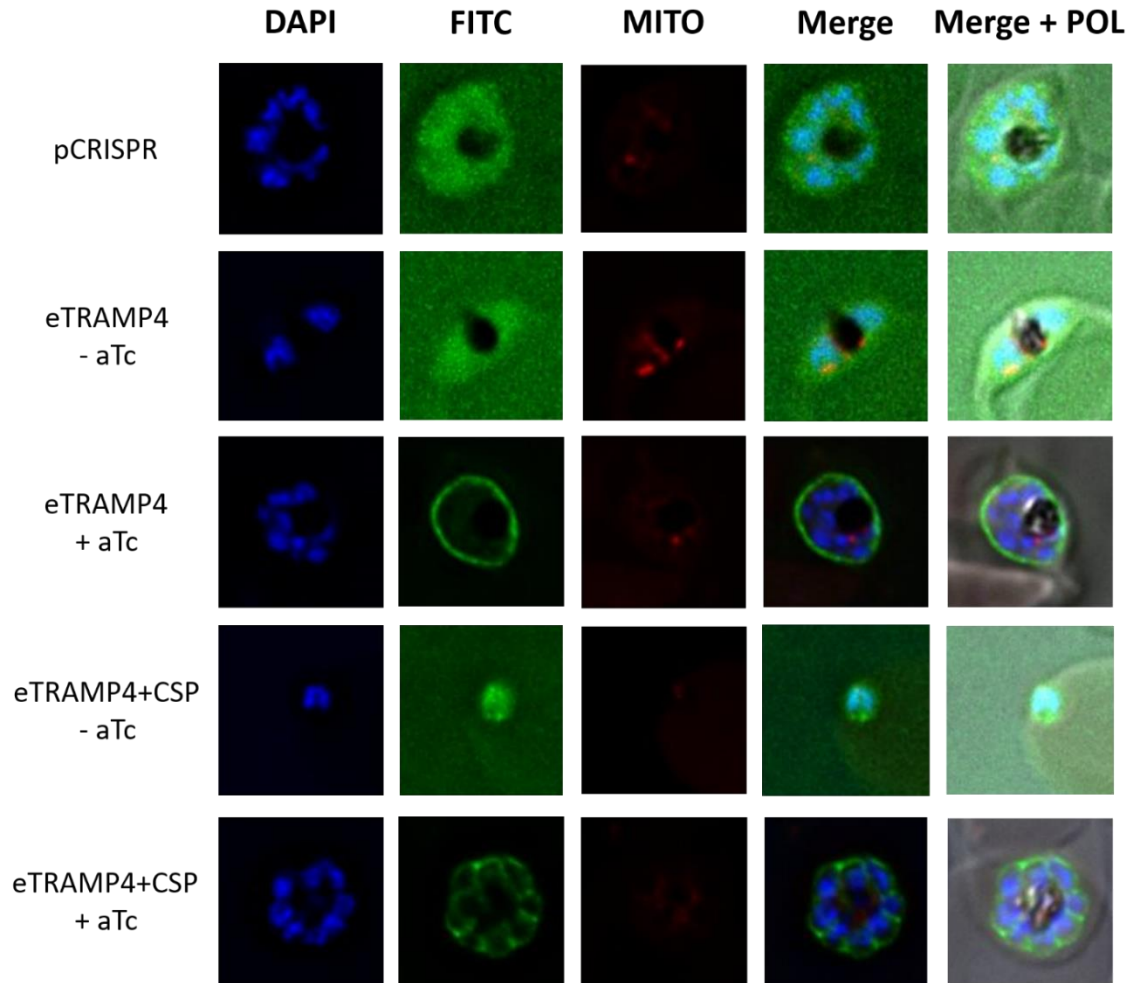
Immunofluorescence assays (IFAs) were performed to determine eTRAMP4-CSP and -P25 antigen subcellular localization by probing for the HA tag at the C-terminal end of the protein scaffold or fusion (**Figure 10**). DAPI stain was used to image the nucleus, FITC shows the HA tag, and MITO shows the mitochondria. There are two types of merged images to contextualize subcellular localization: 1) Merge that overlays DAPI, FITC, and MITO; and 2) Merge + POL that overlays the Merge image on top of a polarized image of the parasite (POL).

The parental pCRISPR parasite line was utilized as a negative control since it does not contain any HA-tagged proteins. Comparing both -aTc conditions of the scaffold and the fusions in the FITC channel to the negative control, there is the same pattern of background signal resulting most likely from over-exposure in the setting of low anti-HA signal. In the eTRAMP4 +aTc condition, there is a ring that forms around early-stage schizont. eTRAMP4-CSP in the +aTc condition also shows a schizont but with a more complex fluorescent pattern: rather than a single solid ring around the whole parasite, there is a partial honeycomb structure that seems to surround the outer portion of the merozoites forming inside the schizont. Based on work done by Hale et al where they examined the PVM during *P. falciparum* egress, they determined that the PVM becomes leaky after schizont segmentation followed by the broken cytoskeleton and PVM shrinking up around the body of merozoites before the parasites are freed<sup>20</sup>. It is our hypothesis that this schizont shown in our eTRAMP4-CSP +aTc IFA image is a very late stage schizont (46-48 hours post-invasion) where the fluorescing PVM has contracted around the merozoites due to breakdown of the cytoskeleton, resulting in the honeycomb-like pattern seen here. Therefore, from these experiments we conclude that in protein-expressing parasites, both our scaffold and fusion to CSP correctly localize to the PVM of the parasite.

While this experiment confirms that the scaffold and the fusions localize to the membranes, the PVM and PPM are closely associated<sup>21-23</sup> and the resolution of IFA cannot resolve if the proteins are expressed on the PVM or PPM. Higher resolution imaging (e.g., immuno-electron microscopy) and host RBC permeabilization IFA studies will be needed to definitively probe display of the CSP (and P25) components from the PVM face in contact with the red blood cell cytosol.

### **Conclusions**

Towards the goal of examining alternative vaccine antigen design strategies, we set out to determine whether model mosquito- and pre-erythrocytic-stage antigens (P25 and CSP, respectively) could be successfully expressed by display from PVM-anchored scaffolds in blood stage parasites. Genetic constructs to achieve this were produced and used to generate viable transgenic parasite lines expressing fusions of these antigens to the PVM-localized eTRAMP4 protein. Expression of full-length fusion protein antigens could be conditionally regulated, and the model antigens tested did not compromise parasite fitness. Altogether, these findings indicate feasibility of stage-ectopic expression of antigens relevant to malaria vaccine development displayed from the PVM of blood stage parasites.



**Figure 10. Immunofluorescence images of parasites in ring or schizont stages in merozoites for 3 parasite lines with and without aTc taken using fluorescent microscopy.** The pCRISPR line, that is the background into which the plasmids are transfected, does not contain the gene for the HA tag that should fluoresce in the FITC channel, and thus serves as a negative control. DAPI = nucleus, FITC = HA tag at the end of the scaffold or fusion, MITO = mitochondria, Merge = merged images, and Merge+POL = merged images overtop a polarized image of the infected RBC.

## Chapter II References

1. Coppi, A. *et al.* The malaria circumsporozoite protein has two functional domains, each with distinct roles as sporozoites journey from mosquito to mammalian host. *J. Exp. Med.* (2011) doi:10.1084/jem.20101488.
2. Scheiblhofer, S. *et al.* Removal of the circumsporozoite protein (CSP) glycosylphosphatidylinositol signal sequence from a CSP DNA vaccine enhances induction of CSP-specific Th2 type immune responses and improves protection against malaria infection. *Eur. J. Immunol.* (2001) doi:10.1002/1521-4141(200103)31:3<692::AID-IMMU692>3.0.CO;2-Y.
3. Heppner, D. G. *et al.* Towards an RTS,S-based, multi-stage, multi-antigen vaccine against falciparum malaria: Progress at the Walter Reed Army Institute of Research. in *Vaccine* (2005). doi:10.1016/j.vaccine.2005.01.142.
4. WHO. *World Malaria Report 2021*. <https://www.who.int/teams/global-malaria-programme/reports/world-malaria-report-2021> (2021).
5. Swearingen, K. E. *et al.* Interrogating the Plasmodium Sporozoite Surface: Identification of Surface-Exposed Proteins and Demonstration of Glycosylation on CSP and TRAP by Mass Spectrometry-Based Proteomics. *PLoS Pathog.* **12**, (2016).
6. Livingstone, M. C. *et al.* In vitro and in vivo inhibition of malaria parasite infection by monoclonal antibodies against Plasmodium falciparum circumsporozoite protein (CSP). *Sci. Reports 2021 111* **11**, 1–15 (2021).
7. Saxena, A. K. *et al.* The essential mosquito-stage P25 and P28 proteins from Plasmodium form tile-like triangular prisms. *Nat. Struct. Mol. Biol.* (2006) doi:10.1038/nsmb1024.
8. Saxena, A. K., Wu, Y. & Garboczi, D. N. Plasmodium P25 and P28 surface proteins: Potential transmission-blocking vaccines. *Eukaryotic Cell* (2007) doi:10.1128/EC.00060-07.
9. Baton, L. A. & Ranford-Cartwright, L. C. Do malaria ookinete surface proteins P25 and P28 mediate parasite entry into mosquito midgut epithelial cells? *Malaria Journal* (2005) doi:10.1186/1475-2875-4-15.
10. Spielmann, T. etramps, a New Plasmodium falciparum Gene Family Coding for Developmentally Regulated and Highly Charged Membrane Proteins Located at the Parasite-Host Cell Interface. *Mol. Biol. Cell* (2003) doi:10.1091/mbc.e02-04-0240.
11. Nasamu, A. S. *et al.* An integrated platform for genome engineering and gene expression perturbation in *Plasmodium falciparum*; *bioRxiv* 816504 (2019) doi:10.1101/816504.
12. Adjalley, S. H. *et al.* Quantitative assessment of Plasmodium falciparum sexual development reveals potent transmissionblocking activity by methylene blue. *Proc. Natl. Acad. Sci. U. S. A.* **108**, (2011).
13. Deitsch, K. W., Driskill, C. L. & Wellems, T. E. Transformation of malaria parasites by the spontaneous uptake and expression of DNA from human erythrocytes. *Nucleic Acids Res.* **29**, 850–853 (2001).
14. Lambros, C. & Vanderberg, J. P. Synchronization of Plasmodium falciparum erythrocytic stages in culture. *J. Parasitol.* **65**, 418–420 (1979).
15. Mackellar, D. C., Vaughan, A. M., Aly, A. S. I., Deleon, S. & Kappe, S. H. I. A systematic analysis of the early transcribed membrane protein family throughout the life cycle of Plasmodium yoelii. *Cell. Microbiol.* (2011) doi:10.1111/j.1462-5822.2011.01656.x.
16. Spielmann, T., Gardiner, D. L., Beck, H. P., Trenholme, K. R. & Kemp, D. J. Organization of ETRAMPs and EXP-1 at the parasite-host cell interface of malaria parasites. *Mol. Microbiol.* (2006) doi:10.1111/j.1365-2958.2005.04983.x.
17. Noe, A. R. *et al.* A full-length Plasmodium falciparum recombinant circumsporozoite protein expressed by Pseudomonas fluorescens platform as a Malaria vaccine candidate. *PLoS One* (2014)

- doi:10.1371/journal.pone.0107764.
18. Sharma, B. & Jaiswal, M. K. The P25 Ookinete Surface Proteins: Homology Modeling and Phylogenetic Relationships. *ISRN Comput. Biol.* (2013) doi:10.1155/2013/391018.
  19. Vermeulen, A. N. *et al.* Sequential expression of antigens on sexual stages of plasmodium falciparum accessible to transmission-blocking antibodies in the mosquito. *J. Exp. Med.* (1985) doi:10.1084/jem.162.5.1460.
  20. Hale, V. L. *et al.* Parasitophorous vacuole poration precedes its rupture and rapid host erythrocyte cytoskeleton collapse in Plasmodium falciparum egress. *Proc. Natl. Acad. Sci. U. S. A.* **114**, 3439–3444 (2017).
  21. Matthews, K. M., Pitman, E. L. & de Koning-Ward, T. F. Illuminating how malaria parasites export proteins into host erythrocytes. *Cellular Microbiology* (2019) doi:10.1111/cmi.13009.
  22. Goldberg, D. E. & Zimmerberg, J. Hardly Vacuous: The Parasitophorous Vacuolar Membrane of Malaria Parasites. *Trends in Parasitology* (2020) doi:10.1016/j.pt.2019.11.006.
  23. Eksi, S. & Williamson, K. C. Protein targeting to the parasitophorous vacuole membrane of Plasmodium falciparum. *Eukaryot. Cell* (2011) doi:10.1128/EC.00008-11.

## Chapter III: Preparing Parasites for Use as a Aseptic Vaccine

### Abstract

Establishing a robust method of isolating intact blood stage parasites from the host erythrocyte has the potential to allow for easy processing of transgenic *Plasmodium falciparum* parasites for final use as a vaccine. Methods of separating infected RBCs from uninfected cells in cultures and isolating parasites from RBCs have been documented in literature before, but have not been used to ensure an intact PVM or quantify remaining RBC material in cultures. We address this by purifying schizonts using Percoll or magnets, removing the RBC using a protease inhibitor, and comparing the purification methods using Giemsa staining, IFAs, and ELISAs. Overall, these comparisons point to magnetic cell separation as a better method to yield higher quality and more quantifiable final product of pelleted schizonts, with room for future work to continue the process of removing further RBC contaminants.

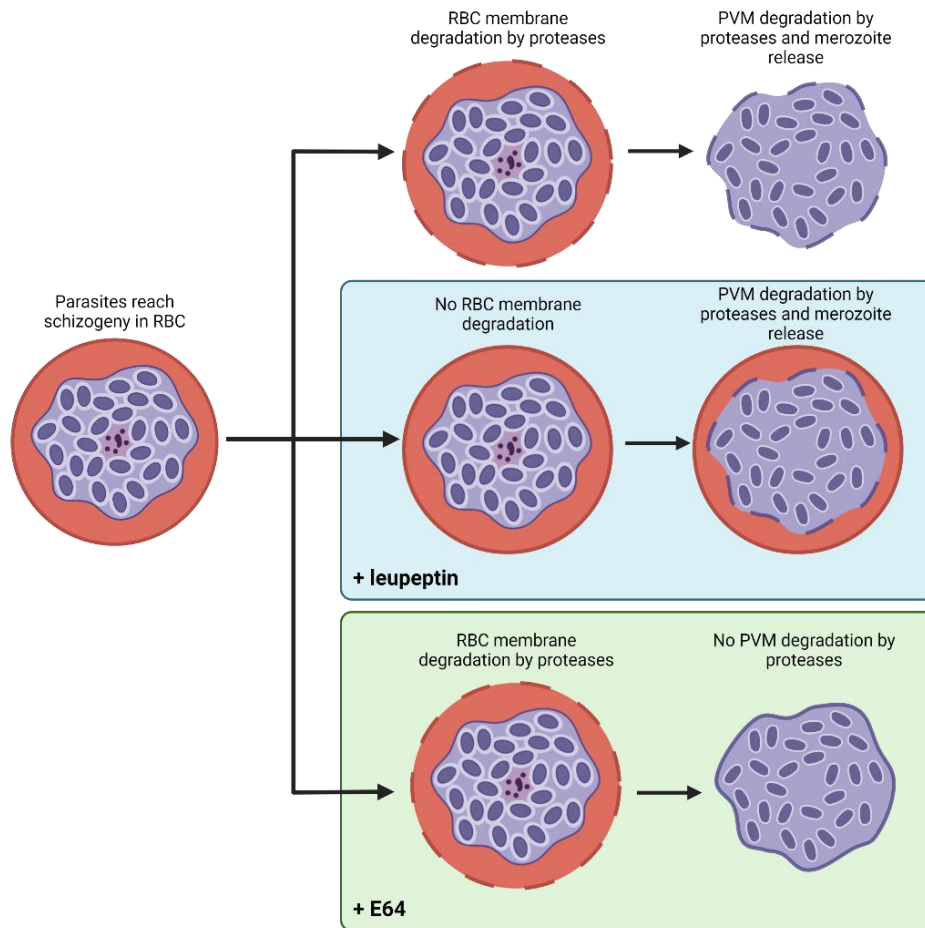
### Introduction

To effectively present antigens and minimize the risk of triggering an  $\alpha$ -RBC immune response, the parasites must first be removed from RBC host with intact PVMs. As RBCs have a light, ghost-like appearance on Giemsa stains when infected with *Plasmodium*, we have termed this idea of removing the RBC and keeping the parasite intact as “de-ghosting”. A gentle process of removing the RBC and separating any remaining RBC material is needed and we can leverage parasite biology to assist in designing a suitable method of de-ghosting. The current understanding of egress involves degradation of the RBC membrane and degradation of the PVM are done via separate proteases. However, inhibiting one set of proteases does not affect the other (**Figure 11**). Examination done by Delplace et al showed that the addition of leupeptin caused disintegration of the PVM while the RBC membrane remained intact<sup>1,2</sup>. Building upon this work, further study done by Salmon et al has shown that using an epoxide-based cytochrome protease inhibitor (shortened as E64) allowed for RBC membrane degradation but arrested PVM proteolysis<sup>3</sup>, forming PVM-enclosed merozoite structures (PEMS).

As the RBC membrane is proteolyzed and dissolved during egress, there is little concern of pure, successfully de-ghosted parasites causing an  $\alpha$ -RBC reaction. However any uninfected erythrocytes or early stage parasites that would not be inhibited by E64 pose a threat of eliciting immune responses against human RBCs. A further purification step before de-ghosting by E64 may limit the amount of these contaminating cells and lower the risk of non-parasite-specific immune responses. We evaluated two methods for selectively enriching parasite-infected RBCs from synchronized cultures, namely, Percoll<sup>4</sup> and magnetic cell separation (MACS)<sup>5,6</sup>. **Figure 12** shows the workflow for Percoll (top) and MACS (bottom). Percoll separation uses gradient centrifugation where uninfected RBCs, rings, trophozoites, and early schizonts are pelleted and late schizonts are isolated at the top of the Percoll gradient. These isolated late schizonts can then thoroughly washed to remove Percoll carry-over. MACS is a column-based magnetic enrichment method that facilitates isolation of parasites with large heme crystals (trophozoite to schizont) based on the paramagnetic properties of the crystalline hemozoin pigment that is formed during parasite maturation<sup>5</sup>. Uninfected erythrocytes, rings, and

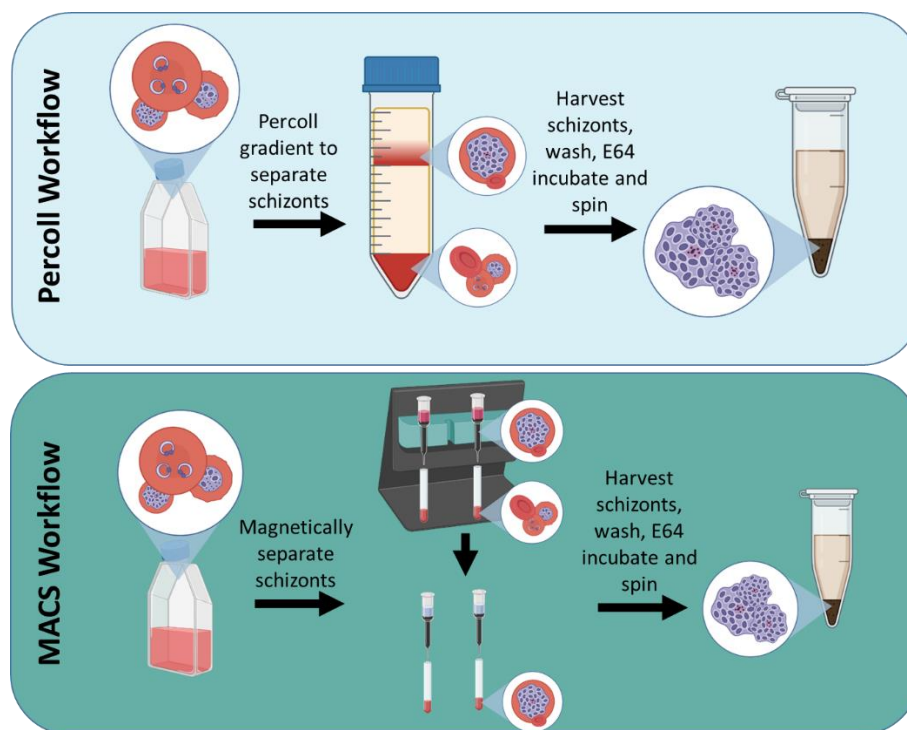
early trophozoites are removed after several washing steps, and late trophozoites and schizonts are eluted upon removal from the magnetic field.

This chapter focuses on de-ghosting transgenic parasites using E64, purifying samples by either Percoll or MACS, and assessing which purification method may be better in terms of reduction of RBC contamination using IFA and ELISA.



**Figure 11. A simplified diagram of the current understanding of parasite egress from RBCs and pathway inhibitions.** (Top) Under normal conditions, parasites at schizogony use two different set of proteases: one set to degrade the RBC membrane and one set to degrade the PVM, which releases merozoites to infect new RBCs. (Middle) With the addition of leupeptin, the degradation of the RBC membrane is inhibited but the PVM degradation is not, resulting in free merozoites within an RBC. (Bottom) With the addition of E64, RBC membranes are degraded as normal but PVM degradation is inhibited, resulting in merozoites trapped within a PVM.





**Figure 12. Graphical representation of Percoll (top) and MACS (bottom) workflows for purification of schizonts for de-ghosting with E64.** Percoll separates schizonts from other cells via discontinuous gradient centrifugation and isolated schizonts are then washed to remove Percoll carry-over. MACS magnetically separates late trophozoites and schizonts from other cells due to their paramagnetic nature, after which they are eluted from the filter and washed to remove any other potential carry-over.

## Methods

Methods herein are presented in the order they were done to achieve final results: initial Giemsa staining, purification, and isolation by E64 (which is followed by another Giemsa stain), followed by either IFA or ELISA.

### Giemsa Staining

Thick-thin blood smears were generated by aspirating media out of settled parasite culture flasks that developed a monolayer on the bottom of the flask. The flask was then tipped and approximately 20 $\mu$ L of parasite culture was placed on the center of a glass slide. Another glass slide was placed on top of the droplet and dragged across to create a parasite gradient smear. The slide was dried at room temperature before fixation in methanol for 1 minute. Slides were then stained in a 5% v/v Giemsa stain solution (Giemsa stain, modified; Millipore Sigma) in deionized water for 20 minutes. Slides were rinsed in water and blotted dry using blotting paper. A droplet of Resolve Immersion Oil (Resolve Immersion Oil, Epredia; VWR) was applied to the slide, a slide cover was applied, followed by another droplet of immersion oil before examination under 100X magnification on a light microscope.

### **Purification of Parasites**

Purified samples of late-stage parasites are generated using modified methods for either by Percoll<sup>4,7</sup> or magnetic cell separation (MACS)<sup>5,6</sup>.

Percoll purification began with 6mL of 65% Percoll ( ) in a 15mL conical tube that served as a stop gradient. Parasite cultures were pelleted at 3200RPM for 5 minutes and then resuspended to 50% hematocrit using wash media. 1 to 4mL of 50% hematocrit parasite culture was carefully layered on top of the Percoll without disturbing the stop gradient. Gradients were spun at 1500g for 10 minutes with no brake. Tubes were removed from the centrifuge and the schizont layer—which settles into a fine layer at approximately 6mL on the conical tube—was removed and transferred into a 50mL conical tube. This schizont pellet was then washed once using wash media and spun at 3200RPM for 5 minutes to remove excess Percoll.

For MACS, a magnetic filter column was assembled with a tap and a 10mL syringe filled with wash media. The column was pre-wetted using wash media and the column was assembled into a custom 3D printed stand at MIT using magnets from K & J Magnets. A reservoir was placed underneath the column and a 0.7mm diameter needle was attached to the tap. Parasite cultures were concentrated to a total volume of 5mL and transferred into the column via serological pipette. The tap was opened and allowed to drip to allow for uninfected RBCs and early stage parasites to pass through. The column was rinsed 4 times by adding 5mL of wash media to the column per wash, without letting the filter dry. Post-rinse, the needle was carefully removed from the tap and the column system (magnetic filter column, tap, and syringe) was removed from the magnet. The column system was placed over a 50mL conical tube and 5mL of wash media was added to the column. The tap was opened and let drip (without drying the filter) to elute out late stage parasites; this elution was repeated once. The tap was then opened and 5mL of wash media from the syringe was injected into the column gently to disturb parasites in the filter before the tap was opened and allowed to drip to further elute late stage parasites; this was repeated once.

### **Isolating Parasites from RBCs using Protease Inhibitor E64**

A working solution of 10 $\mu$ M E-64 protease inhibitor (E64; Millipore Sigma) was made using +ATC/+BSD parasite culture media. Cultures were assessed for 5 to 10% parasitemia of ~44 hours-post-invasion late stage schizonts via Giemsa stain. Culture flasks were then incubated overnight with 10 $\mu$ M E64, +ATC, +BSD media. The following day, cultures were smeared and Giemsa stained to ensure parasites lacked an RBC membrane around PVM-enclosed merozoite structures (PEMS).

### **IFA Staining**

Purified, de-ghosted parasites were centrifuged post-E64 incubation and E64-media was aspirated. Parasites were then washed 3 times with wash media and all wash media was aspirated out. Each parasite pellet was resuspended in 500 $\mu$ L of fixing solution (4% v/v paraformaldehyde and 0.0075% v/v glutaraldehyde in 1X PBS) and rocked at room temperature for 30 minutes. Parasites were pelleted at 8000 g and washed with 1mL of 1x PBS before being resuspended in 500 $\mu$ L permeabilization solution (0.1% v/v Triton X-100 in 1X PBS) and rocked at room temperature for 10 minutes. Parasites

were pelleted at 8000 g and washed with 1mL of 1X PBS. Pellets were then resuspended in 500 $\mu$ L of blocking solution (3% w/v bovine serum albumin in 1X PBS) and rocked at room temperature for 30 minutes. Parasites were pelleted and blocking solution was aspirated before pellets were incubated in 400 $\mu$ L of primary antibody solution (mouse  $\alpha$ -HA primary antibody from Cell Signaling Technology at 1:350 dilution in blocking solution) and rocked overnight at 4°C. Parasites were pelleted and primary antibody solution was aspirated before pellets were incubated in 400 $\mu$ L of secondary antibody solution (Alex Fluor 488-conjugated  $\alpha$ -mouse secondary antibody from Cell Signaling Technology at 1:400 dilution in blocking solution) and rocked for 1 hour at room temperature while protected from light. Parasites were then pelleted and washed in 1X PBS with DAPI (1:1000 DAPI in 1X PBS), rocked for 5 minutes wrapped in foil at room temperature before final pellet and resuspension in 20 to 40 $\mu$ L of 1X PBS. 4 $\mu$ L of sample was transferred onto a slide and dried at 37°C for 10 minutes. 5 $\mu$ L of Prolong Diamond Gold was added to sample, a cover slip was placed, and the slide was dried overnight at 37°C. Final slides were then viewed and imaged using the DeltaVision Elite Widefield Deconvolution imaging system at the W.M. Keck Biological Imaging Facility in the Whitehead Institute.

## ELISA

ELISAs were done using a slightly modified version of the indirect ELISA protocol from Bio-Rad. Purified, de-ghosted parasites were centrifuged post-E64 incubation and E64-media was aspirated. Parasites were then washed 3 times and resuspended in wash media, and distributed across a flat-bottom 96-well plate for each well to result in 100uL. 50uL of wash media are used to fill the rest of the plate. Samples were then serially diluted down the plate using 50uL. 1X BioRad Coating Buffer (BUF030) was added and the plate was incubated overnight at 37°C to dry the cells to the well bottoms. Any remaining coating buffer was gently tapped out onto paper towels. 200uL of BioRad Wash Buffer (BUF031) was added to each well, the plate was upturned onto paper towels and the buffer gently tapped out. This wash was repeated two more times. 150uL BioRad Blocking Solution (BUF032) was added, the plate was incubated for 1 hour at 37°C. The plate was then washed 4 times. Primary antibody was diluted in wash buffer to reach a volume of 100 $\mu$ L per sample well:  $\alpha$ -glycophorin A ( $\alpha$ -GPA; Stem Cell Technologies, FITC-conjugated mouse  $\alpha$ -human CD235a antibody, Clone 2B7) was diluted 1:3000 for detecting RBC membrane contaminants and establishing optical densities for blood standards;  $\alpha$ -circumsporozoite ( $\alpha$ -CSP; mouse antibody 2A10 provided by Dr. Azza Idris of the Ragon Institute) was diluted 1:3000 for detecting CSP presented on the PVM as antigen;  $\alpha$ -P25 ( $\alpha$ -V5; ThermoFisher Scientific, mouse V5 tag monoclonal antibody) was diluted 1:4000 for detecting P25 presented on the PVM as antigen. 100 $\mu$ L of primary antibody solution was added to each well and the plate was incubated for 1 hour at 37°C. The plate was washed 3 times. Secondary antibody was diluted in wash buffer to reach a volume of 100 $\mu$ L per sample well:  $\alpha$ -mouse HRP (goat  $\alpha$ -mouse IgG (H+L) secondary antibody HRP; ThermoFisher Scientific) was diluted 1:3000 for detecting the primary antibody. 100 $\mu$ L of secondary antibody solution was added to each well, the plate was wrapped in foil and incubated for 1 hour at 37°C. The plate was then washed 3 times. 100uL of BioRad HRP substrate solution (BioRad TMB Core+ for HRP-conjugated antibodies) was added to each well, the plate was re-wrapped in foil and incubated at room temperature for 30 minutes. 50 $\mu$ L of stop

solution (0.16M sulfuric acid) was added to each well and the plate's absorbance was read on the SpectraMax M2/M2e microplate reader at a wavelength of 605nm.

### **ELISA Data Analysis**

ELISA data analysis was done using Python code, which is available through a GitHub repository upon request. Data from the SpectraMax M2/M2e microplate reader was imported into a Jupyter notebook. Blood standards were fit using the raw data for a 4-parameter logistic (4PL) curve. Parameters from this 4PL were used to fit sample data to determine the amount of RBC contamination, where sample data was four-fifths of the raw sample data due to normalization of glycophorin A (GPA) present on the PVM surface. As mentioned in the Results section, IFAs showed the presence of GPA on the surface of the PVM and we hypothesized that this is from the ingress of the parasite into the RBC, where the PVM is derived in part from the RBC membrane. Due to approximate surface area ratios where the RBC is 5 times the size of the merozoite on ingress, we are estimating that one-fifth of the GPA signal is due to the GPA on the PVM. Quantification of the RBC contamination was done using an inverse 4PL and plotted with the blood standard curve for comparison.

## **Results and Discussion**

### **Isolating Parasites from RBC Hosts using Protease Inhibitor E64**

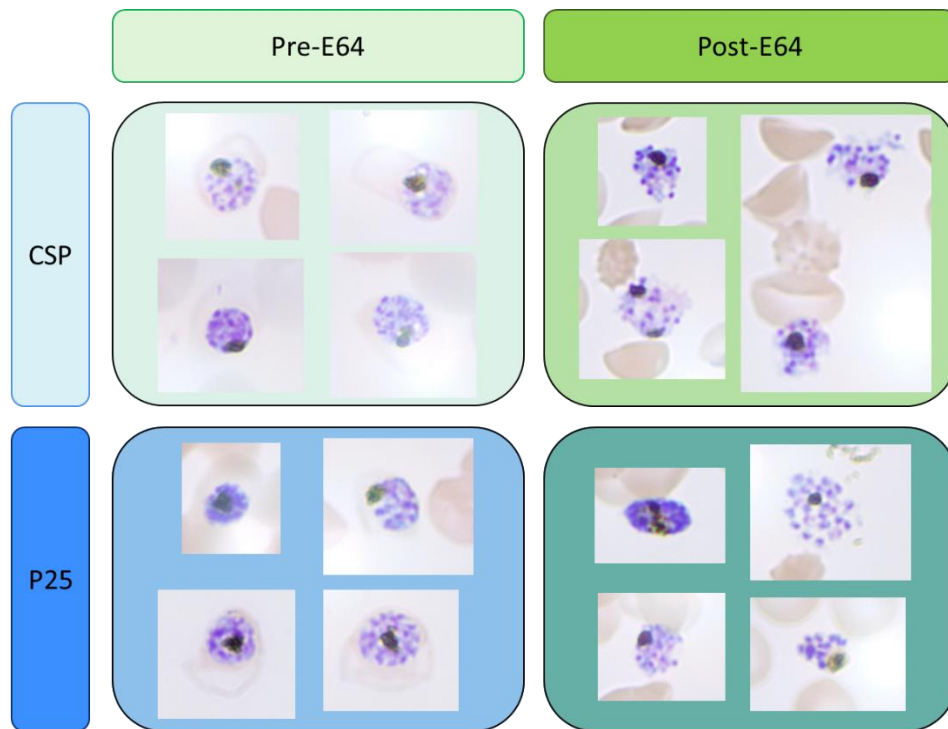
We adapted the method of Salmon *et al* for our studies, and applied 10  $\mu$ M E-64 an asynchronous cultures of CSP- and P25-expressing transgenic parasites where schizonts were at approximately 44 hours post-invasion. After incubating with E-64 for at least 8 hours, cultures were smeared and Giemsa stained to assess formation of PEMS (**Figure 13**). Giemsa is a nucleic acid stain, and parasites appear as a purplish body with dark purple spots for nuclear content and even darker purple spots for the hemozoin crystals that are a byproduct of hemoglobin catabolism. Erythrocytes stain a light pinkish color. For both CSP- and P25-transgenic parasite lines pre-E64 incubation (left column, **Figure 13**), there is a faint pink RBC stain that surrounds the schizont that is not present after addition of E-64 (right column, **Figure 13**). Despite no RBC to encapsulate the schizonts, the general shape of the parasites is still an intact rounded body, highly suggestive of an intact PVM. Thus, we can form PEMS using the protease inhibitor E64.

### **Assessment of Purification via Giemsa Stain**

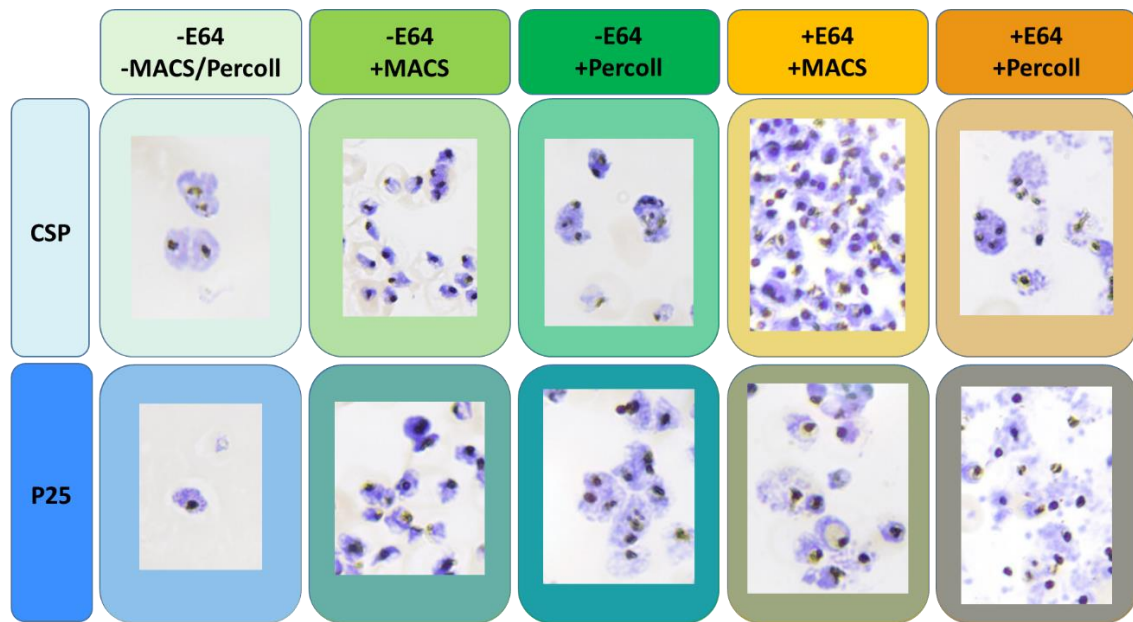
Transgenic schizonts were purified from uninfected RBCs, rings, and most trophozoites using either MACS or Percoll. Parasites were then incubated with E64 for at least 8 hours and Giemsa stained. The results of these stains can be seen in **Figure 14**. In agreement with both our asynchronous experiments (mentioned in the previous subsection) and with work done by Salmon *et al*<sup>3</sup>, parasites were found to form PEMS with exposure to E64, regardless of purification method (**Figure 14**, second and third columns). Parasites under +E64 +MACS conditions seem to have a larger number of parasites compared to +E64 +Percoll, however this is due to MACS purification also magnetizing and isolating late trophozoites in addition to schizonts from culture.

After exposure to E64, it is also clear that there is some parasite shearing occurring in Percoll-purified samples that is not present in MACS-purified samples. Purple debris-like particles that are outside PEMS and are not contained to any solid body. This makes for less clear PEMS formation in Percoll-purified samples compared to MACS.

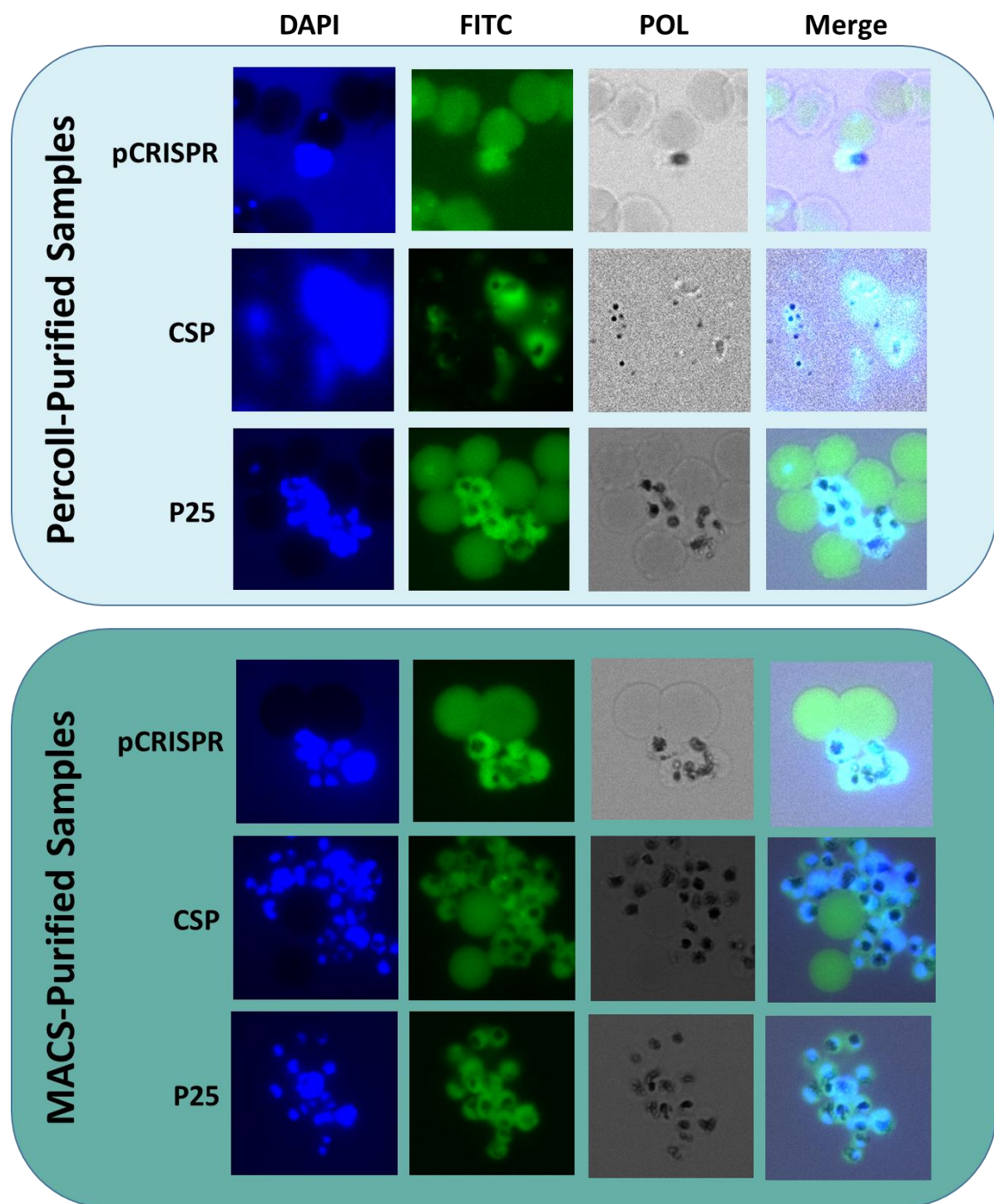
Weighing the two methods via Giemsa stain does not lead to a definite answer on which method might be better for vaccine production. MACS can do larger culture volumes with less parasite shearing but also includes trophozoites, which are non-viable for de-ghosting via E64. Percoll effectively isolates schizonts but seems to shred the limited numbers that are available in a single run. To further elucidate the advantages and disadvantages of each method to determine the optimal path for purification, analysis by IFA and ELISA is explored in the next sections.



**Figure 13. Grid of Giemsa stains for CSP- and P25-transgenic parasites, before and after incubation with 10µM E64 for at least 8 hours.** Parasites stain purple while RBCs stain a light red/brown color. For both parasite lines, before E64 is applied (left column) schizonts can be seen inside erythrocytes. After E64 incubation (right column), schizonts do not have a present RBC surrounding them, akin to the formation of PEMS as seen in Salmon's work.



**Figure 14.** Grid of CSP- and P25-transgenic parasite lines (top and bottom, respectively) pre-purification via MACS or Percoll and pre-exposure to E64, as well as under various combinations of these conditions. MACS-purified parasites have a larger number of parasites by the inclusion of late trophozoites in addition to schizonts, compared to Percoll-purified parasites. Percoll-purified parasites do seem to have more shearing that causes parasite debris not belonging to the enclosed body of a PEMS.



**Figure 15. Comparison between purification methods using immunofluorescent assays.** A two-part grid of immunofluorescence assays (top set = Percoll-purified and bottom set = MACS-purified) done on the parental line pCRISPR (top row), CSP-transgenic parasites (middle row), and P25-transgenic parasites (bottom row) where parasites were stained for nuclear content (far-left column), glycophorin A and the HA tag (middle-left column). Also included are bright field images of the cells (right-middle column) and the three channels merged together (far-right column). DAPI = nuclear content. FITC = glycophorin A and HA tag. POL = bright field image. Merge = all three channels merged.



### Assessment of Purification via Immunofluorescence

After purification, transgenic lines were probed and analyzed using immunofluorescence assays (IFAs) to ensure that parasites were free from RBCs and that PVMs were intact. Samples were purified either by Percoll or MACS. Samples were then probed using DAPI for nuclear content, anti-glycophorin A (GPA) for RBC membranes, and anti-HA for the HA tag at the end of the presented antigen (on the PVM surface). However, due to the unavailability of antibodies at the time of the experiment, both  $\alpha$ -GPA and  $\alpha$ -HA antibodies are fluorescent in FITC. Thus distinguishing the parasites from RBCs will be done using the presence of DAPI and the merged images to assess localization.

**Figure 15** shows two sets of grids for IFAs on transgenic parasite lines: the top grid for Percoll-purified samples and the bottom for MACS-purified samples. In each of the grids, the top row is the parental parasite line pCRISPR that does not express an HA-tag; the middle row are CSP-transgenic parasites; and the bottom row are P25-transgenic parasites. Images shown here are representatives of the whole slide and show an average field of view when looking across the space.

For all MACS-purified samples, there is a clear delineation for nuclear content-containing bodies in the DAPI channel. While some bodies are larger due to the mass of merozoites encapsulated in PVMs and some bodies are smaller punctates from earlier stage schizonts or wider separation between merozoites within a single schizont, there is a clear fluorescent area and dark sections where the RBCs are. Percoll-purified samples do not have the same clear-cut nature, with Percoll P25 being the closest match to the MACS samples. Percoll pCRISPR seems to have some early ring-infected RBCs that show as small punctates that are isolated in a dark body, away from other fluorescent sources that could hint at schizogony. The previously mentioned parasite shearing that could be seen in the Percoll Giemsa stains is also present in the IFAs, notably in the Percoll CSP sample, that causes the non-solid blobs seen in all channels. Other fields of view for Percoll CSP also showed this shearing, and it seems to be present only in Percoll-treated samples.

Across our samples, there is a difference in the amount of RBC contaminants between Percoll- and MACS-purified samples. It seems that Percoll has more RBCs at the IFA stage than MACS, indicated by green circle in FITC that do not co-localize with blue fluorescence in DAPI. While only qualitative in nature, it does hint that MACS might be a better purification technique than Percoll, which can be assessed by more quantitative measures.

There is an important note regarding the overlap of FITC signal due to the available antibodies: pCRISPR samples in both Percoll and MACS light up green in FITC. However, we believe this to be caused by the presence of GPA on the surface of the PVM. Although directly against the results of previous work done by Salmon<sup>3</sup>, our samples--including our control pCRISPR line that does not have an HA tag to fluoresce--still fluoresce when probing using  $\alpha$ -GPA in the FITC channel. Our hypothesis for this is that in the creation of the PVM during egress into an RBC, the PVM takes the RBC membrane as its first iteration of a PVM that later is remodeled as the parasite progresses from ring to trophozoite to schizont. This will be critical for the quantitative analysis of RBC contamination in samples by ELISA.



### Assessment of Purification via ELISA

Alongside the IFAs, indirect ELISAs were performed on the same set of purified parasites. To assess for RBC contamination, parasites were done in 8-point serial dilutions, in triplicate, on a plate with their own 24-point blood standard for normalization and control. Blood standards and parasite samples were probed with  $\alpha$ -GPA at a 1:3000 dilution. Once read on a SpectraMax M2/M2e microplate reader at a wavelength of 605nm, blood standards were fit using their estimated concentrations in a 4-parameter logistic (4PL) curve. Once parameters were found, these parameters were used to calculate the number of RBCs in samples using their measured optical densities via an inverse 4PL.

As mentioned in the IFA section, the control parasites fluorescing in only the presence of  $\alpha$ -GPA leads to the hypothesize that the PVM contains GPA from the RBC host membrane from the merozoite's egress into the RBC. Despite the lack of  $\alpha$ -GPA fluorescence in samples from Salmon, other groups have also found that there is some material carryover from host erythrocyte to parasite for PVM formation on egress<sup>8-11</sup>. While the exact mechanism is not known of what is or is not included, we are using our findings to normalize ELISAs for the amount of GPA present on parasite PVM surface. For this endeavor, we utilized the known surface area of RBCs at  $136\mu\text{m}^2$  and estimated a surface area for a merozoite using a sphere and a cone with a diameter of  $1.25\mu\text{m}$  to be  $25.91\mu\text{m}^2$ . Since the surface area of the RBC is 5 times the size of the merozoite, we estimate that one-fifth of the raw optical density signal originates from the GPA on the PVM, leaving the rest of the signal to be interpreted as contaminating RBCs in the well with parasites.

**Table 2. List of equations for ELISA calculations.** A is the value at 0 cells, D is the value at infinite cells, C is the point of inflection, and B is the Hill coefficient.

<b>4PL</b>	$y = D + \frac{A - D}{1 + (\frac{x}{C})^B}$	<i>Eq. 1</i>
<b>Inverse 4PL</b>	$x = C(\frac{A - D}{y - D} - 1)^{\frac{1}{B}}$	<i>Eq. 2</i>

Using the signal for blood probed with  $\alpha$ -GPA, we then utilized the 4PL formula listed in **Table 2**, Eq. 1 to fit the data for the blood standard and calculate values for the four parts of the equation: A is the minimum value obtained at 0 cells, D is the maximum value obtained at infinite cells, C is the point of inflection, and B is the Hill's slope of the curve. X is the estimated number of cells for any Y optical density. Then using four-fifths of the sample optical density signal and the inverse 4PL from **Table 2**, Eq. 2, we were able to estimate the number of RBCs in a given sample. These curves and estimated numbers of RBC contaminants are shown graphically in **Figure 16** and numerically in **Table 3**.

As with any inverse 4PL to calculate an x from y, an x can only be found when the value of y is between A and D. Therefore if after normalization the optical density of the sample was still above or below the minimum and maximum allowed values, then those values were not used or plotted as the calculated x would not be accurate for the 4PL. Optimally, there would be m = 8 for each sample set.

Smaller *m* values would likely imply there is too much contamination, as values that must be removed are greater than *D*. Taking this into account, there is an apparent trend shown for samples in Table 3. While Percoll samples across the board have smaller ranges per sample, there are far fewer samples able to be calculated as values were still above the maximum value as well as the minimums are either on the order or larger than the MACS minimums. Thus, quantitatively, there is more RBC contamination in Percoll-purified samples than MACS-purified samples, which agrees with our assessment from IFAs and Giemsa stains.

**Table 3. Range of estimated RBCs contaminating parasite samples using inverse 4PL.** *M* is the number of samples that were able to be estimated from optical densities that fell within their respective *A* and *D*.

Sample	Percoll			MACS		
	Minimum	Maximum	<i>m</i>	Minimum	Maximum	<i>m</i>
pCRISPR	$9.89 \times 10^5$	$1.05 \times 10^6$	2	$1.52 \times 10^5$	$1.63 \times 10^6$	6
	-	-	0	$2.25 \times 10^5$	$6.09 \times 10^5$	6
	$1.32 \times 10^6$	$1.93 \times 10^6$	2	$1.36 \times 10^5$	$1.28 \times 10^6$	7
CSP	$1.99 \times 10^5$		1	$1.38 \times 10^5$	$1.56 \times 10^6$	6
	$2.64 \times 10^5$	$4.59 \times 10^5$	2	$1.61 \times 10^5$	$3.59 \times 10^6$	8
	$1.84 \times 10^5$	$8.18 \times 10^5$	3	$1.37 \times 10^5$	$9.32 \times 10^5$	6
P25	$9.69 \times 10^4$	$6.17 \times 10^5$	8	$1.93 \times 10^5$	$4.21 \times 10^5$	8
	$1.37 \times 10^5$	$2.19 \times 10^5$	8	$1.90 \times 10^5$	$3.89 \times 10^5$	8
	$9.01 \times 10^4$	$2.70 \times 10^5$	6	$1.90 \times 10^5$	$3.81 \times 10^5$	8

**Figure 16** shows a grid of 4PLs for Percoll-purified (left column) and MACS-purified (right column) samples of the parental parasite line pCRISPR (top row), CSP-transgenic parasites (middle row), and P25-transgenic parasites (bottom row). Grey triangles are measured optical density values for the blood standard and the grey dotted line is the 4PL fit to those measured values. Blue, purple, and orange circles correspond to the 3 sets of 8-dilution samples from which the measured optical density values were used to estimate the number of RBC cells contaminating the sample. All of the values shown on the graphs are those that fall between their respective *A* and *D* for their standard curve, where samples contain an estimated number of RBCs that are in the upper half of the linear region.

While these graphs alone can be difficult to make direct comparisons, easier comparisons between curves can be seen in **Figure 17**. The top row compares blood standards for pCRISPR, CSP and P25 across both Percoll-purification (top-left) and MACS-purification (top-right), while the bottom row compares the estimated RBC contamination in the samples for both Percoll (bottom-left) and MACS (bottom-right). Directly comparing the blood standards from the top row of **Figure 17**, the Percoll-purified blood standards show a larger breadth between linear regions (shifting of curves left to right) while having much more similar maximum and minimum asymptotes than the MACS-purified blood standards. This can be taken to mean that there is larger plate-to-plate variation between these standards whose parameters could affect the calculation of RBC contamination for Percoll whereas MACS plates generally have a more similar linear region which can make direct comparisons of samples on different MACS plates more clear as they have similar parameters for estimating contamination. Additionally, we can see the difference that the breadth of the Percoll blood standards

have on the spread of Percoll sample data, while MACS blood standards allow for closer comparisons as the data share close linear regions. There is a discrepancy between P25 versus CSP and pCRISPR MACS blood standards, as shown in **Figure 17**. This is most likely due to plate differences in the lower concentrations of blood on the plate and a larger number of cells that adhered or clumping that may have occurred could lead to larger optical density values in the lower regions. Increased lower bounds of optical density (or increased A in the 4PL) could lead to altered linear regions and skewed values for calculating RBC contamination. Repetition of these plates in combination with the use of a plate washer could result in more uniform results or identification of an unknown phenomena for performing ELISAs on whole cells.

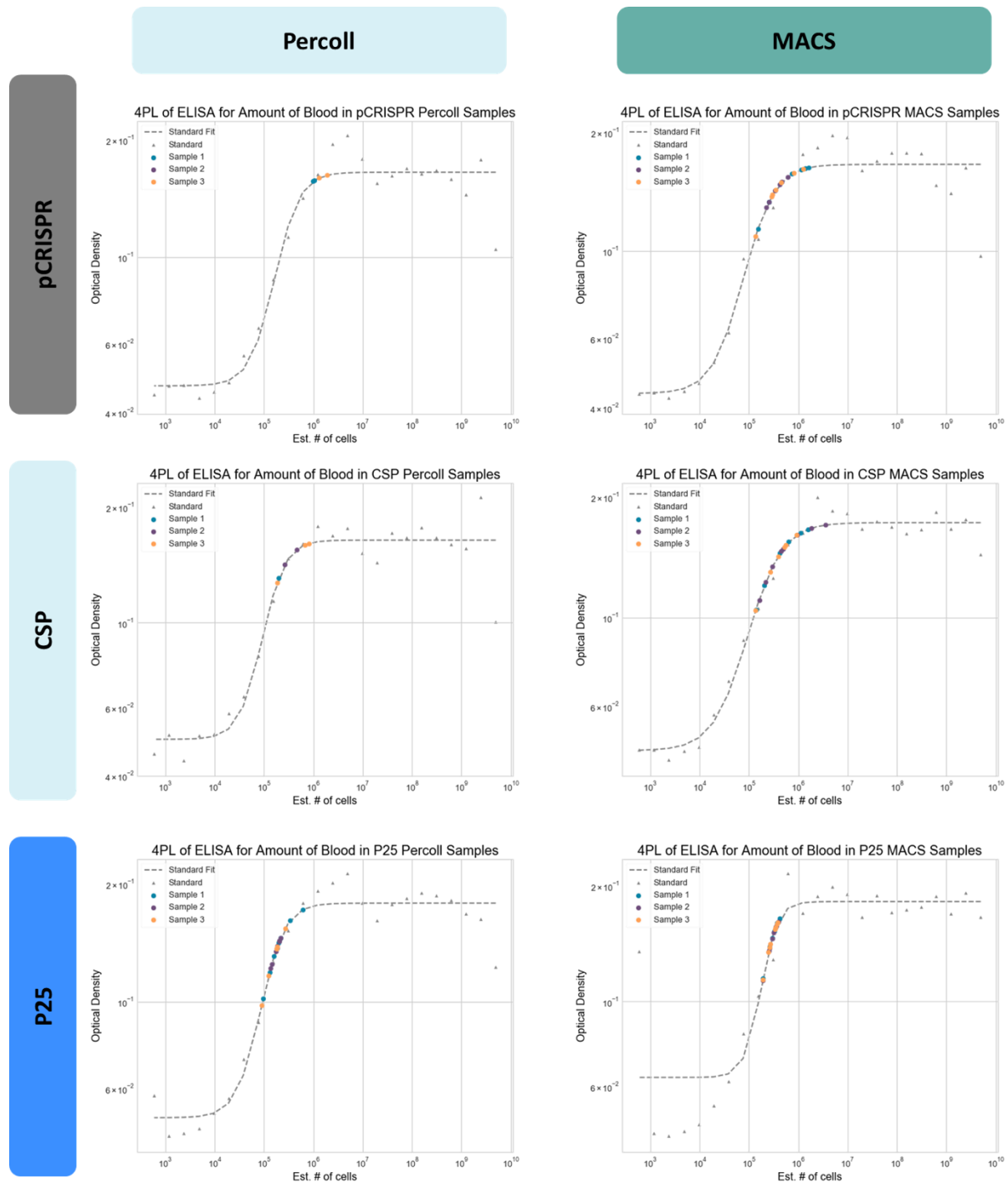
All in all, we take these data to posit that MACS purification yields more intact transgenic parasites with a greater understanding of the amount of RBC contamination in samples in comparison to Percoll-purified parasites. Despite the inclusion of trophozoites due to the magnetic separation, the overall benefits of being able to quantify the number of RBCs still needing to be removed and the larger number of viable parasites for vaccine use outweigh the presence of trophozoites.

To fully maximize the utility of PEMS, further removal of RBC material needs to be done. Although the use of antibodies for purification could mean more effort in terms of large-scale manufacturing, it is necessary to assess many--including non-optimal--different avenues of purification. Additionally, further ELISA analysis using recombinant CSP and P25 to estimate the number of viable PEMS for vaccine use is also critical for upscale and optimization.

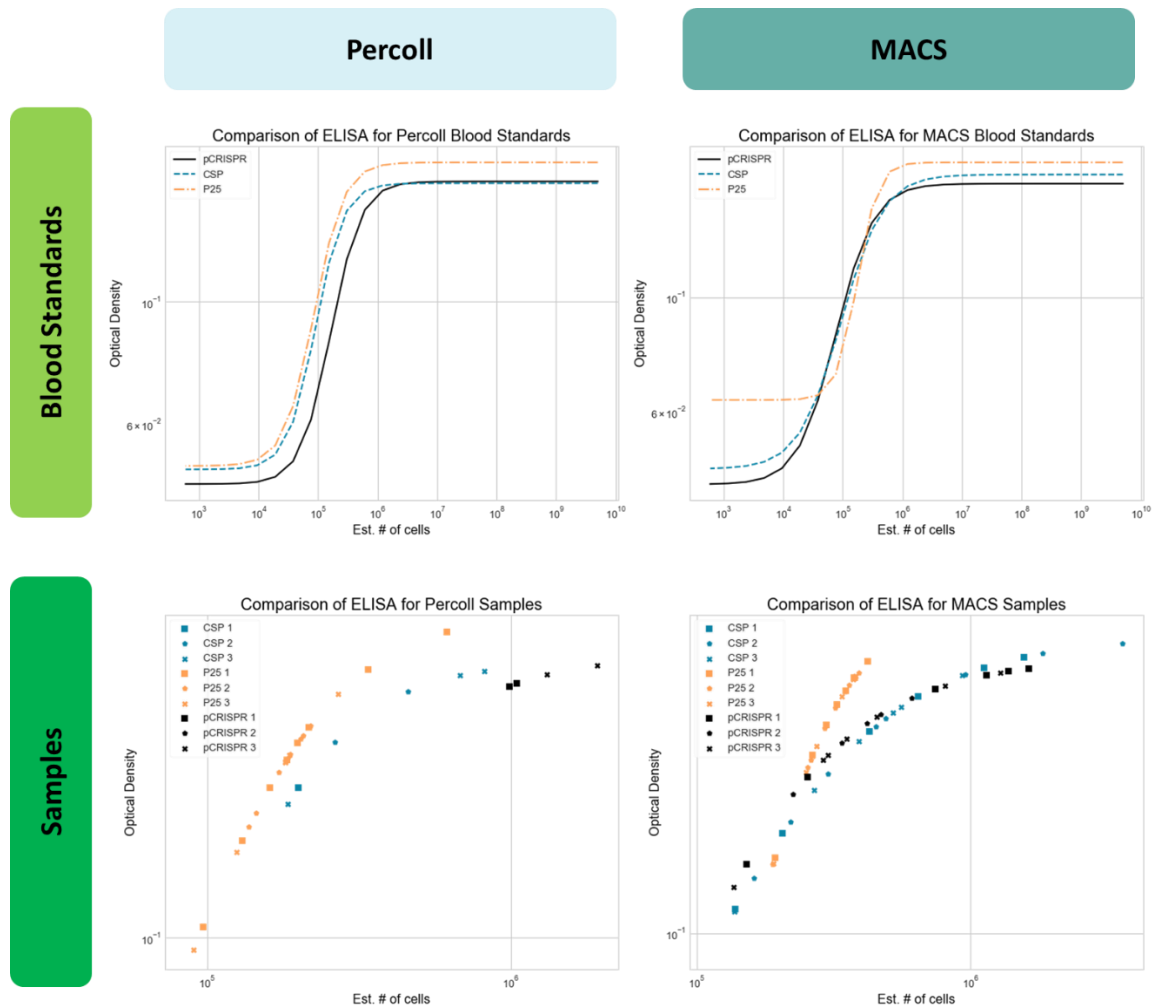
## **Conclusions**

De-ghosting using E64 yields PEMS with intact PVMs, which is critical for antigen presentation on the surface of the parasite. Two purification methods of removing uninfected RBCs and non-de-ghosted parasites from the PEMS have been used and compared, yielding one methodology that proves to be better than the other in terms of Giemsa stains, IFAs, and ELISAs.

Once additional effort has been made to remove excess RBC material and quantify the number of viable PEMS for vaccine usage, animal models to assess immunogenicity and protection via challenge models are the next step to bringing a new malaria vaccine to the clinic.



**Figure 16. Comparisons between blood standard curves and calculated contaminants using 4PL.** A grid of 4-parameter logistic curves for Percoll-purified (left column) and MACS-purified (right column) for parental parasite line pCRISPR (top row), CSP-transgenic parasites (middle row), and P25-transgenic parasites (bottom row). Grey triangles are the measured optical density (OD) values for known blood concentrations and the grey dashed line is the 4PL fitted curve to these points. Samples of parasites ( $n = 3$ ) that have the concentrations calculated by the inverse 4PL are represented by blue, purple, and orange circles. Only sample points that fall within the linear region (between the A and D values of the 4PL) are shown on the graphs.



**Figure 17. Grid of comparisons between different ELISA 4PLs for Percoll-purified (left column) and MACS-purified (right column) samples. Blood standards (top row) are compared between the 4PL curves for pCRISPR (black solid line), CSP (blue dashed line) and P25 (orange dot-dashed line). Samples (bottom row) compare the calculated values for the estimated number of RBCs contaminating parasites, where values are plotted only if their optical density is between their respective A and D.**

### Chapter III References

1. Delplace, P. *et al.* Protein p126: a parasitophorous vacuole antigen associated with the release of *Plasmodium falciparum* merozoites. *Biol. cell* **64**, 215–221 (1988).
2. Debrabant, A. & Delplace, P. Leupeptin alters the proteolytic processing of P126, the major parasitophorous vacuole antigen of *Plasmodium falciparum*. *Mol. Biochem. Parasitol.* **33**, 151–158 (1989).
3. Salmon, B. L., Oksman, A. & Goldberg, D. E. Malaria parasite exit from the host erythrocyte: A two-step process requiring extraerythrocytic proteolysis. *Proc. Natl. Acad. Sci. U. S. A.* (2001) doi:10.1073/pnas.98.1.271.
4. RIVADENEIRA, E. M., WASSERMAN, M. & ESPINAL, C. T. Separation and Concentration of Schizonts of *Plasmodium falciparum* by Percoll Gradients. *J. Protozool.* **30**, 367–370 (1983).
5. Kim, C. C., Wilson, E. B. & Derisi, J. L. Improved methods for magnetic purification of malaria parasites and haemozoin. *Malar. J.* **9**, 1–5 (2010).
6. Ribaut, C. *et al.* Concentration and purification by magnetic separation of the erythrocytic stages of all human *Plasmodium* species. *Malar. J.* **7**, 1–5 (2008).
7. Miao, J. & Cui, L. Rapid isolation of single malaria parasite-infected red blood cells by cell sorting. *Nat. Protoc.* **6**, 140 (2011).
8. Ward, G. E., Miller, L. H. & Dvorak, J. A. The origin of parasitophorous vacuole membrane lipids in malaria-infected erythrocytes. *J. Cell Sci.* **106 ( Pt 1)**, 237–248 (1993).
9. Murphy, S. C. *et al.* Lipid rafts and malaria parasite infection of erythrocytes. *Mol. Membr. Biol.* **23**, 81–88 (2006).
10. Lauer, S. *et al.* Vacuolar uptake of host components, and a role for cholesterol and sphingomyelin in malarial infection. *EMBO J.* **19**, 3556 (2000).
11. Geoghegan, N. D. *et al.* 4D analysis of malaria parasite invasion offers insights into erythrocyte membrane remodeling and parasitophorous vacuole formation. *Nat. Commun.* **2021 121 12**, 1–16 (2021).

## Chapter IV: Conclusions and Future Directions

This work in this thesis developed a proof-of-concept for a new malaria vaccine design that uses a blood stage *Plasmodium falciparum* parasite to present key antigens from the pre-erythrocytic stage or the transmission stage of malaria. Plasmids using a pSN054 backbone for conditional protein expression in parasites was generated using pre-established lab techniques and vectors. Transgenic parasite lines that expressed antigens fused to scaffold proteins were generated and characterized to ensure no growth defects were caused by protein fusion, the correct protein length for fusions, and the proper localization to the PVM. Further work was done to isolate transgenic parasites from their RBC hosts, remove contaminating RBC material from isolated parasites, and quantify any remaining RBC material.

Genetic constructs and viable transgenic parasite lines were produced that could be conditionally regulated, although with some leakiness that was a known issue in the parental line's literature. The protein fusions with model antigens did not compromise parasite fitness and showed localization to the PVM for eTRAMP4-CSP. More work in the future should also examine the localization for eTRAMP4-P25, as it was not able to be included in this thesis.

De-ghosting using E64 yielded parasites outside of RBCs with intact PVMs, which is critical for antigen presentation on the surface of the parasite. Two purification methods of removing uninfected RBCs and non-de-ghosted parasites from the PEMS were compared. Based on the quality of PEMS with minimal shearing to parasites as assessed via Geimsa stain and IFA, the yield via IFA with few RBCs seen in a field of view, and the ability to calculate contaminating RBCs using 4PLs on ELISA data, we posit that MACS is a more appropriate purification method for creating parasites for vaccine usage. While this work requires more optimization for larger throughput and reduced RBC contamination, this sets the groundwork for future studies to be able to use this design and methodology in creating a new malaria vaccine candidate.

Future work will also include *in vivo* immunogenicity studies to assess specific antibody responses to presented antigens and the parasite chassis. Once dosing parameters are identified, challenge models in mice to test the capability of the vaccine design resist infection by the pre-erythrocytic stage, disease severity and elimination during the blood stage, and transmission blocking between hosts by a mosquito vector will be used to quantify protection and potential correlates of protection. A single injectable that is able to elicit humoral responses to two stages in the life cycle would be able fill the void created by malaria rebound that is seen with single-stage vaccine designs, and the data included in this work and works to follow could put those in need in a better position in the fight against malaria.